

1 **All about Nitrite: Exploring Nitrite Sources and Sinks in the Eastern Tropical North**
2 **Pacific Oxygen Minimum Zone**

3

4 John C. Tracey^{1,2}, Andrew R. Babbin³, Elizabeth Wallace¹, Xin Sun^{1,4}, Katherine L. DuRussel^{1,}
5 ⁵, Claudia Frey^{1,6}, Donald E. Martocello III³, Tyler Tamasi³, Sergey Oleynik¹, and Bess B.
6 Ward¹

7

8 ¹ Department of Geosciences, Princeton University, Guyot Hall, Princeton, NJ, USA 08544
9 ² Department of Biology and Paleo Environment, Lamont Doherty Earth Observatory, Columbia
10 University, Palisades, NY, USA 10964
11 ³ Department of Earth, Atmospheric and Planetary Sciences, Massachusetts Institute of
12 Technology, Cambridge, MA, USA 02138
13 ⁴ Department of Global Ecology, Carnegie Institution for Science, Stanford, CA, USA 94305
14 ⁵ Department of Civil and Environmental Engineering, Northwestern University, Evanston, IL,
15 USA 60208
16 ⁶ Department of Environmental Sciences, University of Basel, Bernoullistrasse 30, 4056 Basel,
17 Switzerland

18

19 *Correspondence to:* John C. Tracey (jt16@princeton.edu)

20

21

22

23

24

25

26

27

28

29 **Abstract**

30 Oxygen minimum zones (OMZs), due to their large volumes of perennially deoxygenated
31 waters, are critical regions for understanding how the interplay between anaerobic and aerobic
32 nitrogen (N) cycling microbial pathways affects the marine N budget. Here we present a suite of
33 measurements of the most significant OMZ N cycling rates, which all involve nitrite (NO_2^-) as a
34 product, reactant, or intermediate, in the Eastern Tropical North Pacific (ETNP) OMZ. These
35 measurements and comparisons to data from previously published OMZ cruises present
36 additional evidence that NO_3^- reduction is the predominant OMZ N flux, followed by NO_2^-
37 oxidation back to NO_3^- . The combined rates of both of these N recycling processes were
38 observed to be much greater (up to nearly 200x) than the combined rates of the N loss processes
39 of anammox and denitrification, especially in waters near the anoxic / oxic interface. We also
40 show that NO_2^- oxidation can occur when O_2 is maintained near 1 nM by a continuous purge
41 system, NO_2^- oxidation and O_2 measurements that further strengthen the case for truly anaerobic
42 NO_2^- oxidation. We also evaluate the possibility that NO_2^- dismutation provides the oxidative
43 power for anaerobic NO_2^- oxidation. The partitioning of N loss between anammox and
44 denitrification differed widely from stoichiometric predictions of at most 29% anammox; in fact,
45 N loss rates at many depths were entirely due to anammox. Our new NO_3^- reduction, NO_2^-
46 oxidation, dismutation, and N loss data shed light on many open questions in OMZ N cycling
47 research, especially the possibility of truly anaerobic NO_2^- oxidation.

48

49 **1. Introduction**

50 Nitrogen (N) is essential for life because of its prominent role in DNA, RNA, and protein
51 chemistry. As a result, N limits biological productivity in many marine environments. The

52 dissimilatory biological N loss and recycling pathways are traditionally understood to be strictly
53 separated by O₂ tolerance. The N loss processes of denitrification, the stepwise reduction of
54 NO₃⁻ to N₂, and anaerobic ammonium oxidation (anammox), the oxidation of NH₄⁺ with NO₂⁻ to
55 make N₂, require low O₂ while the N recycling pathways of NH₄⁺ oxidation to NO₂⁻ and NO₂⁻
56 oxidation to NO₃⁻ are viewed as obligately aerobic. Importantly, NO₂⁻ is a product, reactant, or
57 intermediate in all these pathways. Therefore, developing an understanding of NO₂⁻ sources and
58 sinks is essential for a complete understanding of marine N biogeochemistry.

59 Oxygen minimum zones (OMZs) and sediments are the two main marine environments
60 where N loss occurs. There are three major OMZs, the Eastern Tropical North Pacific (ETNP),
61 the Eastern Tropical South Pacific (ETSP), and the Arabian Sea, which occupy 0.1 - 1% of total
62 ocean volume, depending on the O₂ threshold used (Codispoti and Richards, 1976; Naqvi, 1987;
63 Bange et al., 2000; Codispoti et al., 2005; Lam and Kuypers, 2011). Importantly, the OMZ water
64 column is not completely deoxygenated from top to bottom; OMZs are characterized by an
65 oxygenated surface, a depth interval of steeply declining O₂ around the mixed layer depth, called
66 the oxycline, an oxygen deficient zone (ODZ) spanning several hundred meters where O₂
67 declines below the detection limit of common shipboard CTD O₂ sensors, and then a second,
68 gradual, oxycline that transitions to oxygenated deep water. Despite OMZ regions' small size,
69 they are responsible for 30-50% of total marine N loss (DeVries et al., 2013), a magnitude
70 significant for the global marine N budget. In this work, in order to answer several open
71 questions about OMZs and marine N cycling, we conducted a suite of ¹⁵N stable isotope
72 measurements of the most important N cycling microbial pathways in OMZs. We report the N
73 loss rates of anammox and denitrification, as well as the N recycling rates of NO₃⁻ reduction,
74 NO₂⁻ oxidation, and NH₄⁺ oxidation, all of which involve NO₂⁻.

75 A distinctive feature of OMZs is a secondary nitrite maximum (SNM) (Codispoti et al.,
76 2001; Brandhorst, 1959; Codispoti and Packard, 1980). The highest nitrite concentrations within
77 the SNM can reach 10 μM , much higher than the peak values found in the primary nitrite
78 maximum at the base of the photic zone, which average ~ 100 nM globally (Lomas and
79 Lipschultz, 2006). Several recent works have shown or argued that the SNM's NO_2^- is supplied
80 via high rates of the first step of denitrification, NO_3^- reduction to NO_2^- (Lam et al., 2009; Lam
81 and Kuypers, 2011; Kalvelage et al., 2013; Babbin et al., 2017, 2020). NO_3^- reduction has been
82 proposed (Anderson et al., 1982) to be one-half of a rapid loop where NO_3^- and NO_2^- are
83 recycled through simultaneously occurring NO_3^- reduction and NO_2^- oxidation. This loop has
84 been supported through experimental measurements of both rates (Babbin et al., 2017, 2020;
85 Kalvelage et al., 2013; Lipschultz et al., 1990). In this view, elevated NO_3^- reduction also
86 generates NH_4^+ , via organic matter (OM) remineralization, which enhances anammox at the
87 expense of denitrification in oxycline and upper ODZ waters (Babbin et al., 2020). In this study,
88 we conducted tests to further document this rapid loop's existence and role in enhancing
89 anammox.

90 Recent measurements of NO_2^- oxidation have returned significant rates from both the
91 oxycline and the ODZ, findings that challenge the paradigm that NO_2^- oxidation is an obligately
92 aerobic process. Evidence for high, widespread NO_2^- oxidation rates in low O_2 waters has
93 accumulated from direct rate measurements via ^{15}N tracers (Füssel et al., 2011; Lipschultz et al.,
94 1990; Peng et al., 2015, 2016; Ward et al., 1989; Kalvelage et al., 2013; Tsementzi et al., 2016;
95 Sun et al., 2017, 2021a; Babbin et al., 2017, 2020), models (Buchwald et al., 2015), and ^{15}N
96 natural abundance measurements (Casciotti et al., 2013). Many explanations have been
97 proposed including microaerophilic nitrite oxidizing bacteria (NOB) adapted to low but non-zero

98 O₂ conditions (Penn et al., 2016; Bristow et al., 2016; Tsementzi et al., 2016; Bristow et al.,
99 2017) where the O₂ for these NOB is transiently supplied to previously deoxygenated waters by
100 (1) vertical or horizontal mixing of the ocean surface or nearby oxic water (Casciotti et al., 2013;
101 Tiano et al., 2014; Bristow et al., 2016; Ulloa et al., 2012), even into the anoxic ODZ
102 (Margolskee et al., 2019; Monreal et al., 2022), or (2) a cryptic O₂ cycle where low-light adapted
103 phototrophs produce O₂ that is consumed by NOB (Garcia-Robledo et al., 2017; Fuchsman et al.,
104 2019).

105 Despite the power of these explanations, they do not preclude the possibility of
106 widespread NOB capable of truly anaerobic NO₂⁻ oxidation, especially in waters from the deep,
107 dark, and deoxygenated ODZ core. This possibility is bolstered by sequencing data that show
108 the presence of an NOB metagenome assembled genome (MAG) with a preference for the
109 deoxygenated ODZ core in the ETSP (Sun et al., 2019) and ODZ core kinetics experiments
110 where O₂ concentrations above 5 μM inhibit NO₂⁻ oxidation (Sun et al., 2021a). Here we build
111 on past stable isotope experimental results by performing additional depth profile experiments
112 with purged waters from the ODZ *and* O₂ manipulation ¹⁵N tracer experiments across a gradient
113 of O₂ concentrations from 1 nM to 10 μM. Our O₂ manipulation experiments, unlike previous
114 studies, were conducted in vessels that were continuously purged throughout each incubation
115 with a precisely calibrated mixture of N₂, O₂, and CO₂. This experimental design allowed us to
116 continuously maintain low O₂ conditions. In addition, our oxygen concentrations in these assays
117 were verified via a LUMOS sensor, a sensor class with a detection limit of 0.5 nM O₂ (Lehner et
118 al., 2015). Together, these method improvements convincingly show that the O₂ contamination
119 observed to occur in Niskin sampling (Garcia-Robledo et al., 2016, 2021) is removed and that
120 vanishingly low O₂ is maintained throughout the experiment.

121 Anaerobic NO_2^- oxidation would require an alternative oxidant other than O_2 . Many
122 candidates have been proposed (Sun et al., 2023) for this oxidant including IO_3^- (Babbin et al.,
123 2017), Mn^{4+} , Fe^{3+} (Sun et al., 2021a), the anammox core metabolism (Sun et al., 2021a), the
124 observed reversibility of the nitrite oxidoreductase enzyme (Wunderlich et al., 2013; Kemeny et
125 al., 2016; Koch et al., 2015; Buchwald and Wankel, 2022), and NO_2^- dismutation (Babbin et al.,
126 2020; Füssel et al., 2011; Sun et al., 2021a). Due to multiple considerations such as very low
127 IO_3^- in the ODZ core (Moriyasu et al., 2020), low favorability of Mn^{4+} or Fe^{3+} mediated NO_2^-
128 oxidation at marine pH values (Luther, 2010), low anammox rates that do not explain the
129 observed stoichiometry of NO_2^- oxidation to anammox (Kalvelage et al., 2013; Babbin et al.,
130 2020; Sun et al., 2021a), and the inability of the enzyme hypothesis to account for structural and
131 phylogenetic differences in the NXR of the four NOB genera (Buchwald and Wankel, 2022;
132 Sun et al., 2019), we conducted experiments to test the remaining most plausible hypothesis:
133 NO_2^- dismutation.

134 NO_2^- dismutation (Eq. (R4)) is energetically favorable (Strohm et al., 2007; Van de
135 Leemput et al., 2011) although it has not been detected in nature. The reaction is proposed to
136 occur in three steps (Eq. (R1-3)) (Babbin et al., 2020) and DNA sequences that encode possible
137 enzymes for steps two and three (Eqs. (R2, R3)) have been found in ODZ core metagenomic
138 reads and MAGs (Padilla et al., 2016; Babbin et al., 2020). While these sequences were not
139 classified as NOB, they do indicate that parts of the pathway could occur in OMZs. If
140 discovered in OMZs, NO_2^- dismutation would be another N loss pathway, albeit one
141 indistinguishable from denitrification since the ^{15}N atoms in $^{30}\text{N}_2$ come from $^{15}\text{NO}_2^-$ in both
142 pathways. Here we evaluate the hypothesis that NO_2^- dismutation is a significant mechanism for
143 NO_2^- oxidation under low O_2 , by searching for product inhibition, the inhibition of both NO_2^-

144 oxidation and $^{30}\text{N}_2$ production (i.e. denitrification) in response to addition of NO_3^- , substrate
145 stimulation (increases in both $^{30}\text{N}_2$ production and NO_2^- oxidation in response to addition of
146 $^{15}\text{NO}_2^-$), and by comparing the NO_2^- oxidation to the produced $^{30}\text{N}_2$ ratio. A ratio near the 3:1
147 stoichiometry of dismutation ($3 \text{NO}_3^- : 1 \text{N}_2$, Eq. (R4)) would indicate that dismutation could
148 explain the NO_2^- oxidation measured in the ODZ core.



153 A final area of OMZ biogeochemistry that we investigate is the relative balance between
154 anammox and denitrification and these pathways' relationships to the rapid NO_2^- oxidation /
155 NO_3^- reduction loop. After the discovery of anammox, many OMZ studies (Kavelage et al.,
156 2013; Kuypers et al., 2005; Hamersley et al., 2007; Jensen et al., 2011; Thamdrup et al., 2006;
157 Lam et al., 2009), but not all (Ward et al., 2009; Bulow et al., 2010; Dalsgaard et al., 2012) have
158 reported that anammox is the dominant N loss flux in OMZs, a surprising difference from the
159 stoichiometric based prediction that OMZ N loss should be at most 29% anammox (Dalsgaard et
160 al., 2003). While the first wave of these studies did not realize that vial septa were introducing
161 O_2 into the incubations, many studies after this discovery observed the same result (Kavelage et
162 al., 2013; Jensen et al., 2011; Babbin et al., 2020). The prediction of a 29% anammox partition
163 assumes that all NH_4^+ for anammox was derived from remineralization of OM with a mean
164 marine C:N ratio through complete denitrification of NO_3^- to N_2 (Dalsgaard et al., 2003, 2012).
165 Anammox rates exceeding 29% of total N loss would therefore require an additional source of
166 NH_4^+ beyond current observations of denitrification and the resulting NH_4^+ remineralization.

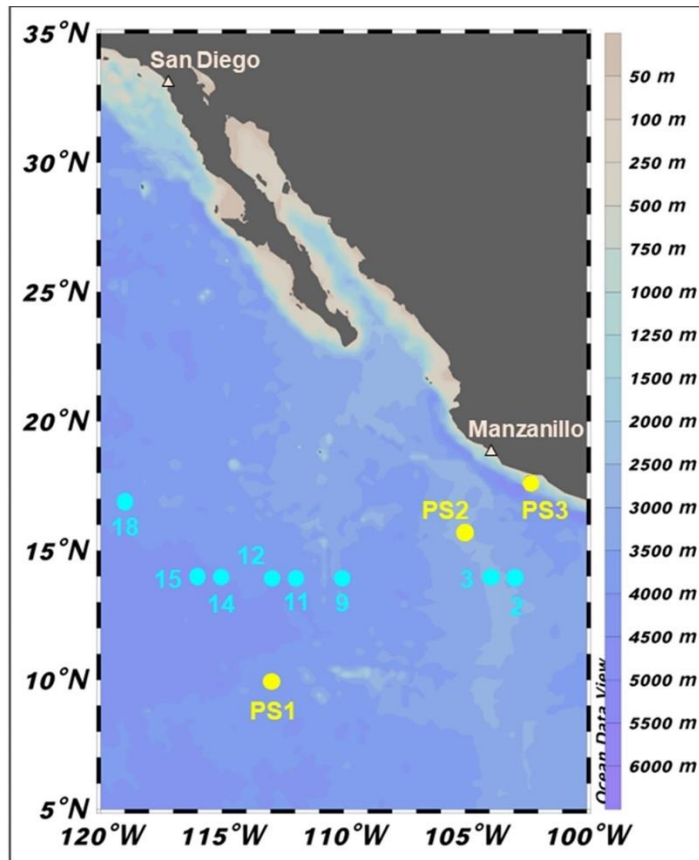
167 The best supported explanations for elevated anammox are that (1) denitrification is the
168 NH_4^+ source, but that complete denitrification peaks episodically in response to OM quality
169 while anammox occurs at a slow, consistent, low rate (Ward et al., 2008; Thamdrup et al., 2006;
170 Babbin et al., 2014; Dalsgaard et al., 2012). The snapshots afforded by isotopic incubations on
171 cruises could therefore easily miss episodes of high complete denitrification. (2) Denitrifiers
172 have a strong preference for particles (Ganesh et al., 2013, 2015; Fuchsman et al., 2017) and
173 CTD samples do not capture marine particles very well (Suter et al., 2017). As a result,
174 differences from the expected percent N loss partition in water column samples are due to
175 missing denitrifiers. (3) The rapid loop between NO_3^- and NO_2^- described previously functions
176 as an “engine” to generate NH_4^+ for anammox at the expense of denitrification. The observed
177 magnitudes of NO_3^- reduction and NO_2^- oxidation and these processes’ ability to produce NH_4^+
178 from the remineralization of OM with standard C:N ratios without complete denitrification make
179 this an additional logical hypothesis.

180 The third hypothesis, the $\text{NO}_2^-/\text{NO}_3^-$ loop, is supported by several pieces of evidence.
181 Firstly, ‘omics studies have revealed widespread modular denitrification in OMZs (Sun et al.,
182 2021b; Ganesh et al., 2015; Fuchsman et al., 2017). Furthermore, experimental studies have
183 shown that as NO_3^- reduction increases near the coast, anammox rates also increase (Kalvelage et
184 al., 2013). Our study’s considerable number of data points, as well as our ability to compare
185 results to rate measurements obtained from identical methods on previous cruises offers a unique
186 chance to test both the variable denitrification and rapid loop hypotheses for elevated anammox
187 rates.

188 OMZs are essential regions for the marine N cycle; however, the biogeochemistry of
189 OMZs may currently be in flux due to anthropogenic pressures. Observational studies have

190 reported decreases in O_2 across the Pacific (Ito et al., 2017) and the expansion of denitrification
191 and anoxia in the ETNP (Horak et al., 2016). Modeling studies suggest that OMZ volume will
192 continue to grow in the near future, with uncertain impacts (Stramma et al., 2008; Keeling et al.,
193 2010; Busecke et al., 2022). As a result, it is important to develop a thorough understanding of
194 OMZ N cycling to be able to predict any changes in marine productivity as deoxygenated
195 regions grow. This study contributes towards this goal through examining four open research
196 questions in OMZ biogeochemistry:

- 197 (1) Is the rapid cycle hypothesis correct, i.e., that NO_3^- reduction and NO_2^- oxidation rates are
198 much greater than N loss rates, especially in the oxycline and ODZ top?
- 199 (2) Does truly anaerobic NO_2^- oxidation occur in OMZ regions?
- 200 (3) If yes, is NO_2^- dismutation the mechanism by which it occurs?
- 201 (4) Is anammox the dominant N loss flux? If yes, what is the explanation?



202

203 **Figure 1:** Sampling locations during 2018 cruises to the ETNP OMZ. SR1805 stations (spring
 204 2018) are shown in yellow while FK180624 (summer 2018) stations are shown in cyan. Stations
 205 PS1 and 18 are located in more oxic environments on the boundary of the OMZ region. The
 206 remaining FK180624 stations occur along a gradient towards the center of the OMZ region,
 207 represented by stations PS2 and FK180624 stations 2 and 3. These three stations are referred to
 208 as OMZ core stations. Station PS3 (referred to as coastal) represents a final biogeochemical
 209 subregion due to its proximity to the coast.

210

211 2. Methods

212 2.1 NO_2^- , NO_3^- , and NH_4^+ concentration measurements

213

Nutrient measurements on all cruises were conducted as follows. Ambient NO_2^-

214

concentrations were measured on each vessel using the sulfanilimide and NED colorimetric

215

technique with a spectrophotometer (Strickland and Parsons, 1972). NO_3^- profile samples were

216

frozen onboard each ship, then thawed and measured immediately using the chemiluminescence

217

method upon return to the Ward laboratory (Braman and Hendrix, 1989). Ambient NH_4^+

218 concentrations were measured on each ship using the OPA method (Holmes et al., 1999; Taylor
219 et al., 2007; ASTM International, 2006). In some cases, NO_2^- and NH_4^+ were measured on
220 different casts than those of the rate measurements. In these cases, figures and calculations use
221 interpolated nutrient values based on the potential density of nutrient sampling and rate
222 measurement depths. Interpolations were performed with the Matlab pchip function.

223 **2.2 NH_4^+ oxidation and NO_3^- reduction rates**

224 Incubation experiments were performed on board the R/V *Sally Ride* in March and April
225 2018 (SR1805). NH_4^+ oxidation and NO_3^- reduction rates were measured at three stations: PS1
226 (open ocean OMZ boundary), PS2 (open ocean, OMZ), and PS3 (coastal OMZ) (Fig. 1). Rates
227 were measured throughout the water column at ten depths per station (see supplemental Table S1
228 for depths). Water was directly sampled from the CTD into 60 mL serum vials. After
229 overflowing three times, bottles were sealed with a rubber stopper and crimped with an
230 aluminum seal. After this, a 3 mL headspace of He was introduced and samples from below the
231 oxygenated surface depths were purged for 15 min with He at a flow rate of 0.4 L min^{-1} . This
232 flow rate exchanged the volume of each bottle one hundred times. Immediately after this, 0.1
233 mL of tracer solution was added to all bottles. $^{15}\text{NH}_4^+$ and $^{15}\text{NO}_3^-$ tracers were added to reach
234 final concentrations of $0.5 \mu\text{M}$ and $3 \mu\text{M}$, respectively. Five bottles were incubated per time
235 course and incubations were ended at 0 (one bottle), 12, and 24 hours (two bottles each) via
236 addition of 0.2 mL of saturated ZnCl_2 . Samples were analyzed at the University of Basel using a
237 custom-built gas bench connected by a Conflow IV interface to a Delta V plus IRMS (Thermo
238 Fisher Scientific). Five mL of the sample were used to convert NO_2^- to N_2O using the azide
239 method (McIlvin and Altabet, 2005). A linear increase of $^{15}\text{N-NO}_2^-$ over time, along with a

240 standard curve to convert from peak area units to nmol N was used to calculate the NO_2^-
241 production rates according to Eq. (5) and (6) below,

$$242 \text{ Ammonium oxidation rate} = \frac{d \text{ }^{15}\text{NO}_2^-}{dt (F_{\text{NH}_4^+})} \quad (5)$$

$$243 \text{ Nitrate reduction rate} = \frac{d \text{ }^{15}\text{NO}_2^-}{dt (F_{\text{NO}_3^-})} \quad (6)$$

244 where:

245 $\frac{d \text{ }^{15}\text{NO}_2^-}{dt}$ is the slope of $^{15}\text{NO}_2^-$ produced over time and

246 $F_{\text{NH}_4^+}$ and $F_{\text{NO}_3^-}$ are the fraction of the NO_3^- and NH_4^+ pools that are labelled with ^{15}N .

247 The significance of the rates was evaluated using a Student's t test with a significance level of
248 0.05. The reported error bars are the standard error of the regression. The NH_4^+ oxidation rates
249 reported here were previously published and the experimental method used is more thoroughly
250 described in this previous publication (Frey et al., 2022).

251

252 **2.3 Anammox and denitrification rates depth profiles**

253 Incubation experiments were performed during SR1805 in March and April 2018 and on
254 the R/V *Falkor* (FK180624) during June and July 2018. As above, rates were measured at PS1,
255 PS2, and PS3 at ten depths per station (see Supplementary Table S1 for sampling depths) during
256 SR1805. On FK180624, rates were measured at eight stations that spanned a gradient from the
257 core of the OMZ region to its edges (see Supplementary Table S2 for sampling depths). At all
258 stations and depths water was directly sampled from the CTD into 320 mL borosilicate ground
259 glass stoppered bottles. After overflowing three times, bottles were stoppered with precision
260 ground glass caps specifically produced to prevent gas flow. The bottles were transferred to a

261 glove bag and amended with the following treatments: 3 μM each of $^{15}\text{NO}_2^-$ and $^{14}\text{NH}_4^+$
262 (denitrification and anammox) and 3 μM each of $^{15}\text{NH}_4^+$ and $^{14}\text{NO}_2^-$ (anammox) on SR1805. 2
263 μM amendments of $^{15}\text{NO}_2^-$ and $^{14}\text{NH}_4^+$ were used on FK180624. It should be noted that at many
264 depths our tracer additions were far above in situ values. Due to this, all anammox and
265 denitrification rates with high changes from baseline nutrient concentrations represent potential
266 rates. Eight mL of tracer amended seawater was aliquoted into 12 mL exetainers (Labco).
267 Exetainers were sealed in a glove bag with butyl septa and plastic screw caps that had been
268 stored under helium for at least one month, removed and then purged for 5 min at 3 psi with
269 helium gas to remove any O_2 that accumulated during sampling and processing. This step is
270 another reason our anammox and denitrification rates sourced from partially or fully oxygenated
271 waters should be regarded as potential rates.

272 Rates for each sampled depth were calculated using a five-timepoint time course with
273 three replicates at each point. Incubations were ended by injecting 50 μL saturated ZnCl_2 and
274 vials were stored upside down to prevent the headspace from leaking through the vial cap during
275 storage and transit. Six months after the cruise, samples were analyzed using a Europa 22-20
276 IRMS (Sercon). Raw data values were corrected for instrument drift due to run position and
277 total N_2 mass. Drift corrected values and standard curves to convert from peak area units to
278 nmol N_2 were used to calculate rates according to the equations below (Thamdrup et al., 2006;
279 Thamdrup and Dalsgaard, 2000, 2002) (for more details see supplemental material),

280 Denitrification (from $^{15}\text{NO}_2^-$)

281 Denitrification Rate =
$$\frac{d\ ^{30}\text{N}_2}{dt(F_{\text{NO}_2^-})^2} \quad (7)$$

282 Anammox (from $^{15}\text{NO}_2^-$)

283
$$\text{Anammox Rate} = \frac{d^{29}\text{N}_2}{dt F_{\text{NO}_2^-}} - 2D(1 - F_{\text{NO}_2^-}) \quad (8)$$

284 Anammox (from $^{15}\text{NH}_4^+$)

285
$$\text{Anammox Rate} = \frac{d^{29}\text{N}_2}{dt F_{\text{NH}_4^+}} \quad (9)$$

286 where:

287 $\frac{d^{30 \text{ or } 29}\text{N}_2}{dt}$ is the slope of the regression of the amount of $^{30 \text{ or } 29}\text{N}_2$ vs. time,

288 $F_{\text{NO}_2^-}$ and $F_{\text{NH}_4^+}$ are the fraction of the NO_2^- and NH_4^+ pools labelled as ^{15}N , and

289 D is the denitrification rate calculated according to Eq. (7).

290 A Student's t test with a significance level of 0.05 was used to evaluate all rates. The reported
 291 error bars are the standard error of the regression. Since the anammox rates measured via both
 292 tracers on the SR1805 cruise were similar in magnitude (Supplementary Table S3), anammox
 293 values reported in Figs. 2, 3, 6, 7, 8, and 9 are based on a combination of these values (see
 294 supplementary material for more information). Previously published (Babbin et al., 2020)
 295 anammox and denitrification rates are sourced from four stations occupied during the R/V
 296 *Thomas G. Thompson's* March and April 2012 cruise to the ETNP (TN278) and the RVIB
 297 *Nathaniel B. Palmer's* June and July 2013 ETSP cruise (NBP1305) and were conducted in the
 298 same manner as the SR1805 and FK180624 incubations. Crucially, the same mass spectrometer
 299 was used to measure N loss rates across the 2012, 2013, and 2018 cruises. Station locations for
 300 the 2012 and 2013 cruises were as follows: TN278 ETNP coastal (20° 00' N, 106° 00' W),
 301 ETNP offshore (16° 31' N, 107° 06' W) and NBP1305 ETSP coastal (20° 40' S, 70° 41' W),
 302 ETSP offshore (13° 57' S, 81° 14' W).

303

304 2.4 SR1805 NO₂⁻ oxidation depth profiles

305 Nitrite oxidation depth profiles were measured in the same exetainers used to measure
306 anammox and denitrification depth profiles (¹⁵NO₂⁻ treatment only). The rate of NO₂⁻ oxidation
307 was determined by converting the NO₃⁻ produced during the incubations to N₂O using the
308 denitrifier method (Weigand et al., 2016; Granger, J., & Sigman, 2009) (see supplemental
309 material for methods details). The samples were stored at room temperature in the dark until
310 analysis on a Delta V (Thermo Fisher Scientific) mass spectrometer that measures the isotopic
311 content of N in N₂O (Weigand et al., 2016). Samples were corrected for instrument drift due to
312 run position and total N₂ mass (for more details see supplemental materials). Drift corrected
313 δ¹⁵N values and a standard curve were then used to calculate the rate as follows,

$$314 \frac{{}^{15}\text{N}}{{}^{14}\text{N}} = \frac{\left[\frac{\delta^{15}\text{N}}{1000} + 1 \right] \times 0.003667}{1 - 0.003667} \quad (10)$$

$$315 \text{NO}_2^- \text{ ox. rate} = \frac{d \left[{}^{44}\text{N}_2\text{O}_{\text{area}} \times \frac{{}^{15}\text{N}}{{}^{14}\text{N}} \right]}{dt F_{\text{NO}_2^-}} \quad (11)$$

316 where Eq. (10) is a rearrangement of the definition of δ¹⁵N:

$$317 \delta^{15}\text{N} = \left[\frac{\frac{{}^{15}\text{N}}{{}^{14}\text{N}}_{\text{sample}}}{\frac{{}^{15}\text{N}}{{}^{14}\text{N}}_{\text{air}}} - 1 \right] \times 1000 \quad (12)$$

318 and ⁴⁴N₂O_{area} is the amount of ⁴⁴N₂O measured as sample peak area in V · sec. 0.003667 is the
319 natural abundance of ¹⁵N in air. A Student's t test with a significance level of 0.05 was used to
320 evaluate all rates. Reported error bars are the standard error of the regression. Previously
321 published (Babbin et al., 2020) NO₂⁻ oxidation rates are from the previously mentioned TN278
322 and NBP1305 cruises and were conducted at the same four stations where N loss rates were

323 measured. These NO_2^- oxidation rate measurements were conducted according to the same
324 procedures used for the SR1805 depth profiles.

325

326 **2.5 NO_2^- oxidation and O_2 manipulation experiments**

327 Experiments were conducted during cruises SR1805 and FK180624 in spring and
328 summer 2018. Wide-mouthed Pyrex round media bottles (800 mL total volume, 500 mL
329 working volume; Corning, USA; product code 1397-500) were used for all incubations. These
330 bottles were modified to include three stainless steel bulkhead fittings (Swagelok, USA) secured
331 to the interior of the lid with a Viton rubber gasket and stainless-steel washer between the lid and
332 the sealing nut. The three ports consisted of two one-eighth inch fluidic ports (inflow and
333 outflow) and one one-quarter inch sampling port. The fluidic ports were fitted with one-eighth
334 inch nylon tubing, with the inflow line penetrating to the base of the bottle. The one-quarter inch
335 sampling port had a butyl rubber septum between the Swagelok stem and nut. This setup
336 permitted *continuous* gas purging of the bottles while maintaining an otherwise closed system.

337 For each depth and O_2 treatment, three bottles were filled to 500 mL with sample water
338 from a Niskin bottle and closed. Sample water for all experiments except station 18 on the
339 FK180624 cruise was drawn from water below 2.2 μM O_2 (See Table S4 for all ambient O_2
340 values). Highly precise digital mass flow controllers (Alicat) were then used to establish the
341 desired O_2 concentrations in each bottle. Mixing ratios were calculated to create a range of O_2
342 concentrations spanning 1 nM, 10 nM, 100 nM, 1 μM , and 10 μM . The gas mixture modified by
343 the mass flow controllers was a zero-air gas mixture (Airgas) consisting of 21% O_2 and 79% N_2
344 and 1000 ppm pCO_2 (the approximate in situ value). Initial gas flow was 1 L min^{-1} for 1 hour to
345 equilibrate the seawater followed by 100 mL min^{-1} for the remainder of the experiment. Bottles

346 were daisy-chained together to maintain the same flow rate among them (two bottles on SR1805,
347 six on FK180624). As in the depth profile experiments, $3 \mu\text{M } ^{15}\text{NO}_2^-$ amendments were added
348 prior to purging. Incubations were conducted in the dark at 12°C in a cold room (SR1805) or
349 beverage cooler (FK180624). At the beginning of the experiments, after purging for one hour,
350 O_2 was checked with a LUMOS optode with a detection limit of 0.5 nM (Lehner et al., 2015) and
351 CO_2 was checked by measuring pH using the colorimetric meta-cresol purple method. The
352 LUMOS optode confirmed that O_2 concentrations were within a few nM of the calculated values.
353 While our use of high precision digital mass flow controllers and this qualitative O_2 check
354 provide confidence that our O_2 concentrations are accurate, due to the fact that O_2 was not
355 continuously monitored through the time course, we refer to each O_2 concentration as a
356 “putative” concentration for the remainder of this manuscript. Samples (50 mL) were withdrawn
357 every 12 hours for two days with a four inch hypodermic needle attached to a 60 mL disposable
358 plastic syringe. Samples were ejected into acid-cleaned HDPE bottles pre-amended with $200 \mu\text{L}$
359 of saturated ZnCl_2 solution. Bottles were screwed closed and wrapped with parafilm. Samples
360 from each of the three initially collected bottles were collected to create triplicates at each time
361 point.

362

363 **2.6 NO_2^- dismutation experiments**

364 Nitrite dismutation experiments were performed during SR1805 at Station PS3 (coastal
365 waters) at two deoxygenated depths: 60 m and 160 m . Incubations were performed in the same
366 manner as the above anammox, denitrification, and NO_2^- oxidation experiments where all three
367 rates were measured in the same exetainers. Experiments consisted of eight total treatments:
368 four varying $^{15}\text{NO}_2^-$ tracer concentrations ($1.125, 5.25, 10.5, \text{ and } 20.25 \mu\text{M}$ for 160 m and $0.75,$

369 1.5, 3.75, and 7.5 μM for 60 m) and two $^{14}\text{NO}_3^-$ treatments (0 or 20 μM). As above, both $^{30}\text{N}_2$
370 and NO_3^- production via the denitrifier method (Weigand et al., 2016) were measured. In order
371 to test our hypothesis that, if dismutation is occurring, the unexplained NO_2^- oxidation rate (the
372 difference between the measured NO_2^- oxidation and the NO_2^- oxidation due to anammox) and
373 the denitrification rate (i.e. the $^{30}\text{N}_2$ production rate) should have a 3:1 ratio, a previously
374 published anammox stoichiometry (Eq. (4) (Kuenen, 2008)) was used to calculate the NO_2^-
375 oxidation due to anammox. The anammox rates used for this calculation are included in the
376 supplementary material (Fig. S4).

377

378 **2.7 Calculation of N loss from NH_4^+ oxidation**

379 The calculation of the maximum possible N loss from NH_4^+ oxidation via NO
380 disproportionation by ammonium oxidizing archaea (AOA) in Supplementary Table S5 was
381 carried out by dividing the measured NH_4^+ oxidation rate by two in accordance with the
382 stoichiometry of NH_4^+ oxidation and NO disproportionation proposed in a previous study (Kraft
383 et al., 2022). It should be noted that this operation represents the extreme case where all $^{15}\text{NO}_2^-$
384 produced in NH_4^+ oxidation is converted to N_2 . We acknowledge this as an unrealistic
385 assumption used to evaluate the extreme limits of the amount of total N loss attributable to NH_4^+
386 oxidation. This operation was carried out for all depths where NH_4^+ oxidation, anammox, and
387 denitrification rates were measured, irrespective of O_2 concentration.

388

389 **2.8 Redundancy analysis (RDA), Principle component analysis (PCA), and statistics**

390 All RDA, PCA, redundancy, and correlation analyses were performed with the available
391 packages in R (v4.2.1 “Funny-Looking Kid”) (R: A language and environment for statistical

392 computing). All data were first normalized around zero before calculating the Pearson's
 393 correlation coefficient. Gene abundances (*nirS* and *amoA*) from qPCR analyses used for the
 394 RDA and correlation analyses were measured as previously described (Peng et al., 2015;
 395 Jayakumar et al., 2009; Tang et al., 2022).

396

397 **2.9 Definition of shallow boundary and ODZ core nomenclature**

398 In the results and discussion sections, results are classified as shallow boundary or ODZ
 399 core waters according to a previously published threshold (Babbin et al., 2020) where shallow
 400 boundary samples have an in situ potential density < 26.4 . This method is based on a global
 401 profile of OMZ waters meant to delineate shallow boundary samples as waters that are oxic or
 402 may be influenced by O₂ intrusions (the surface, the oxycline, and the ODZ top) from those that
 403 are not normally influenced by O₂ intrusions (ODZ core). Due to the fact that the potential
 404 density threshold is based on a global average, a few depths that are clearly in the deep oxycline
 405 based on the SR1805 O₂ depth profiles are classified as ODZ core ($\sigma_{\theta} > 26.4$) by the potential
 406 density threshold. Despite this caveat we used this naming scheme throughout the remainder of
 407 the manuscript to enable comparisons to previous literature (Babbin et al., 2020).

Depth	σ_{θ}	OMZ features	O ₂ intrusions?
Shallow boundary waters	< 26.4	Surface, oxycline, ODZ top	Yes
ODZ core	> 26.4	ODZ core	No

408

409 **Table 1:** Explanation of shallow boundary waters and ODZ core potential density based
 410 nomenclature (Babbin et al., 2020).

411

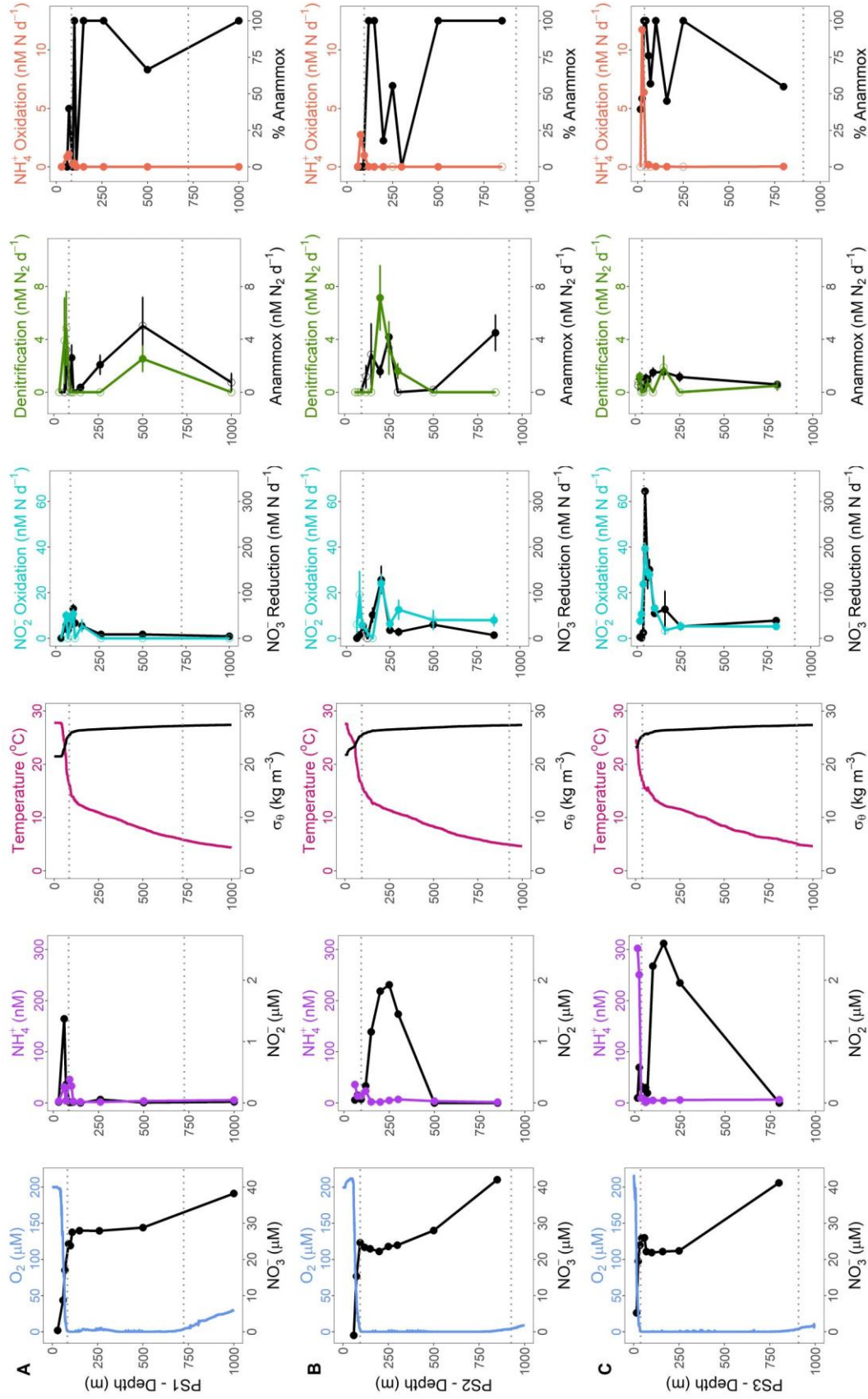
412 **3. Results**

413 **3.1 2018 depth profiles of all N cycling rates**

414 N cycling depth profile experiments were conducted on two cruises (SR1805 and
 415 FK180624) during spring and summer 2018. These two cruises sampled stations along a

416 gradient from the edge of the OMZ region to near the coast. Physical and chemical conditions
417 varied among stations PS1, PS2, and PS3 on the SR1805 cruise (spring 2018) and across all
418 FK180624 stations (summer 2018) (Fig. 2, Fig. S1). Broadly speaking, the vertical span of the
419 ODZ increased and the top of the ODZ shoaled as distance to shore decreased. Deep SNM were
420 observed at almost all stations with the only exceptions being the furthest offshore stations,
421 stations 11 and 18 from the FK180624 cruise (Fig. S1) and station PS1 from SR1805 (Fig. 2A).
422 Peak NO_2^- values for all SNM were on the lower side of the range of previous ETNP
423 observations (Horak et al., 2016), between 1.4 – 2.6 μM .

424 Of the five N cycling processes measured on the SR1805 cruise, NO_3^- reduction rates had
425 the greatest magnitude at most depths. This trend was most pronounced within the upper ODZ,
426 where NO_3^- reduction rates peaked at station PS2, and the oxycline where NO_3^- reduction rates
427 peaked at stations PS1 and PS3 (Fig. 2). Rates of NO_2^- oxidation closely tracked NO_3^- reduction
428 in distribution; in fact, peak NO_2^- oxidation rates co-occurred with peak NO_3^- reduction rates at
429 all three SR1805 stations, reaching maxima of ~ 40 (NO_2^- oxidation) and ~ 300 (NO_3^- reduction)
430 nM N d^{-1} at PS3. However, the magnitudes of NO_2^- oxidation rates were usually lower than
431 NO_3^- reduction rates, sometimes by as much as eightfold. The third N recycling process, NH_4^+
432 oxidation, peaked at or above the oxycline, with peaks of 10 nM N d^{-1} or less. NH_4^+ oxidation
433 was consistently measured to be zero or near-zero throughout the rest of the water column.
434



436 **Figure 2:** SR1805 depth profiles of physical parameters and N cycling rates. **(A)** From left to
437 right, O₂ (μM) and NO₃⁻ (μM) respectively in blue and black, NH₄⁺ (nM) and NO₂⁻ (μM)
438 respectively in purple and black, temperature (°C) and σ_θ (kg m⁻³) respectively in pink and black,
439 NO₂⁻ oxidation and NO₃⁻ reduction rates (nM N d⁻¹) respectively in cyan and black, anammox
440 and denitrification rates (nM N₂ d⁻¹) respectively in black and green, NH₄⁺ oxidation rates (nM
441 N d⁻¹), and percent anammox respectively in coral and black for station PS1 (offshore). **(B)** As
442 above but for station PS2 (OMZ). **(C)** As above but for station PS3 (coastal). Rates that are
443 significantly different from zero are shown as filled circles, open circles signify rates not
444 significantly different from zero. Error bars are the standard error of the regression. Grey dotted
445 lines indicate upper and lower ODZ boundaries at the time of sampling.

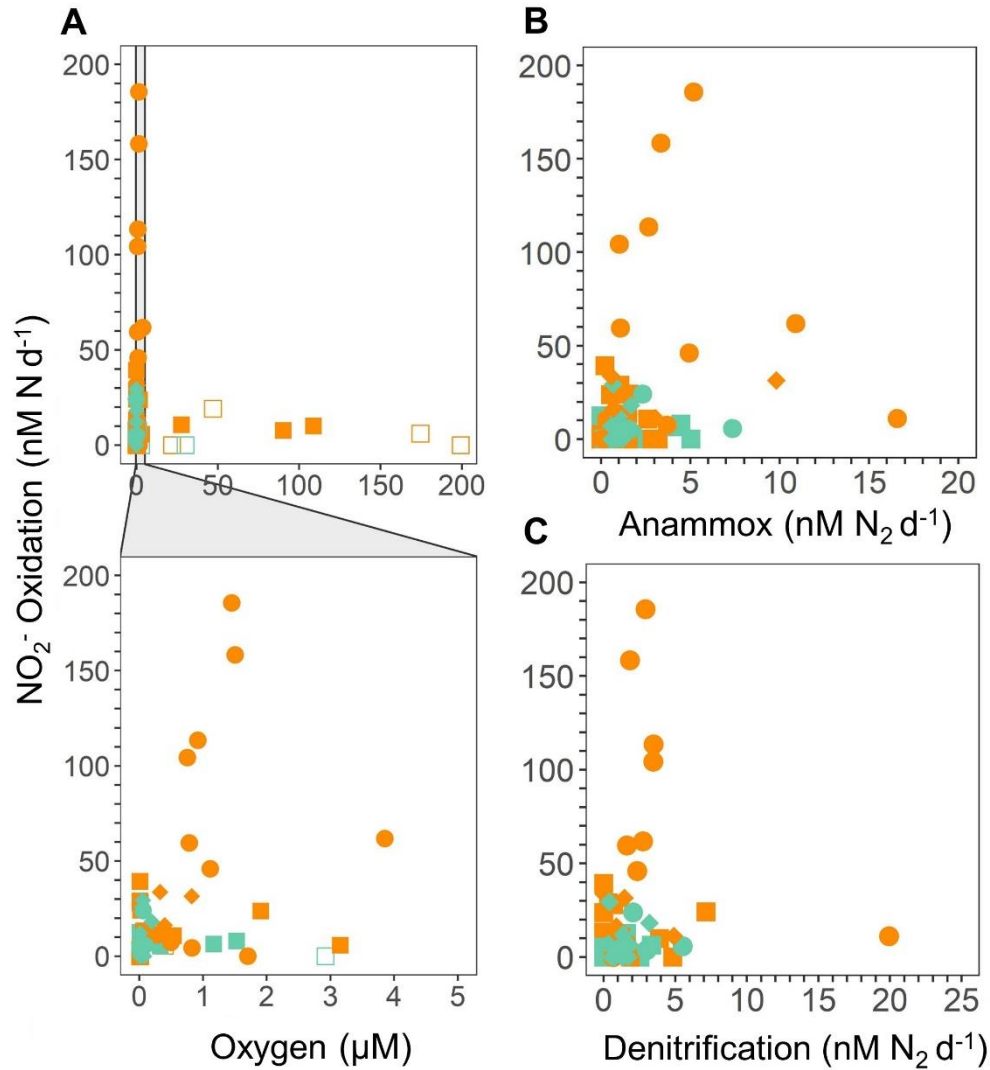
446
447 Across all SR1805 and FK180624 stations, the magnitude of the N loss processes of
448 anammox and denitrification was almost always less than 10 nM N₂ d⁻¹, a much lower magnitude
449 than the N recycling processes of NO₃⁻ reduction and NO₂⁻ oxidation. Like NO₃⁻ reduction and
450 NO₂⁻ oxidation, the two N loss rates peaked in the upper ODZ or right at the oxycline in all three
451 SR1805 stations, although a deep peak (850 m) in anammox was observed at station PS2 (Fig.
452 2B). This peak occurred near the bottom of the ODZ at an O₂ concentration of 1.5 μM. N loss
453 rates also peaked near the oxycline in the three FK180624 stations with broad coverage of the
454 ODZ water column, stations 2, 9 (6 July sampling), and 9 (9 July sampling) (Fig. S1). The
455 relative balance between the two N loss processes as measured by percent anammox varied
456 widely across the water column but largely deviated from the expected partitioning of at most
457 29% anammox (Dalsgaard et al., 2003, 2012). A striking example of this is that 100% anammox
458 values were observed in both ODZ core and shallow boundary (see Table 1 for definitions)
459 samples at many of the SR1805 and FK180624 stations (Fig. 2, Fig. S1).

460

461 **3.2 Anaerobic NO₂⁻ oxidation and O₂ manipulation experiments**

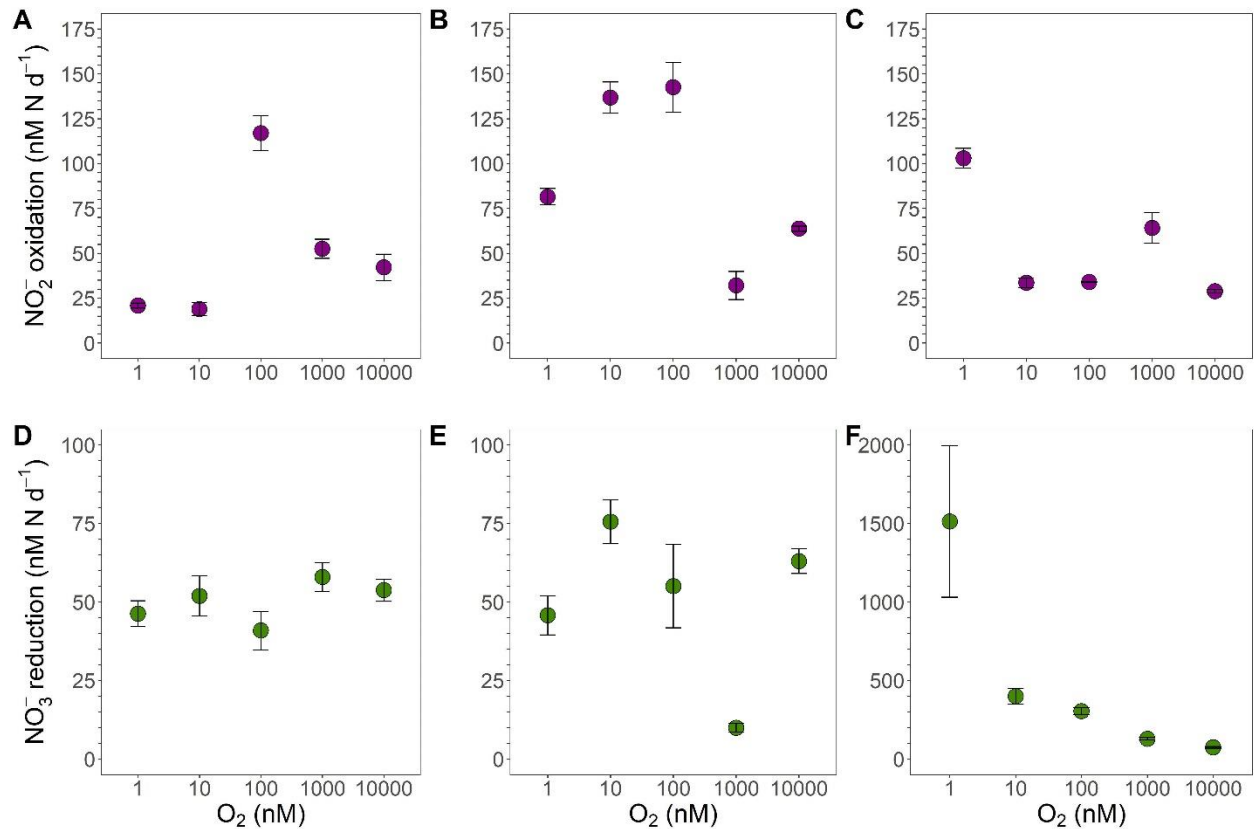
462 Significant NO₂⁻ oxidation rates were detected in depth profiles across a range of suboxic
463 O₂ concentrations (1 – 5 μM) (definition from (Berg et al., 2022)) across all SR1805 stations,
464 often at the same depths and in the same vials where the obligately anaerobic processes of

465 anammox and denitrification were occurring (Fig. 2, Fig. 3A-C, Fig. S2). In order to
466 contextualize our observations, we compared our results to previously published measurements
467 from the TN278 and NBP1305 cruises performed with identical procedures (Babbin et al., 2020).
468 The highest rates were observed in shallow boundary waters across all three cruises (Fig. 3A-C,
469 Fig. S2). Since low but significant levels of O₂ can still support aerobic NO₂⁻ oxidation, a series
470 of O₂ manipulation experiments was carried out on both the SR1805 (spring) and FK180624
471 (summer) 2018 cruises (Fig. 4A-F and Fig. S3). In these experiments, anoxic conditions were
472 checked using a LUMOS O₂ optode with a detection limit of 0.5 nM (Lehner et al., 2015). We
473 observed significant NO₂⁻ oxidation, as well as NO₃⁻ reduction at putative concentrations as low
474 as 1 nM. Notably, compared to previous experiments, gas flushing was constant, with a refresh
475 time of 8 min, so as to maintain O₂ levels within the incubation even while organisms were
476 respiring. At 1nM, O₂ is so scarce that such waters are usually classified as functionally anoxic,
477 for example, a recent review paper defined 3 nM as the threshold below which O₂ cannot play
478 biological or biogeochemical roles (Berg et al., 2022). As a result, these experiments present
479 convincing additional evidence for the occurrence of NO₂⁻ oxidation up to ~100 nM N d⁻¹ at O₂
480 concentrations too low to support aerobic metabolisms.
481



482
 483
 484
 485
 486
 487
 488
 489
 490
 491
 492

Figure 3: NO_2^- oxidation rates (nM N d^{-1}) from the 2018 SR1805 (squares), 2012 ETNP TN278 (circles), and 2013 ETSP NBP1305 (diamonds) cruises vs. (A) O_2 concentration (μM) from shipboard CTD sensors, (B) anammox rates ($\text{nM N}_2 \text{d}^{-1}$), and (C) denitrification rates ($\text{nM N}_2 \text{d}^{-1}$). O_2 concentrations were normalized across cruises. In A, rates that are significantly different from zero as assessed via a Student T-test (p value < 0.05) are displayed as filled symbols, while insignificant NO_2^- oxidation rates are shown as open symbols. Rates measured in shallow boundary waters are colored orange while rates from the ODZ core and below are colored teal. 2012 and 2013 data are republished (Babbin et al., 2020).



493
494

495 **Figure 4:** Oxygen manipulation experiments that show NO_2^- oxidation (purple) (A-C) and NO_3^-
496 reduction (green) (D-F) rates (nM N d⁻¹) measured across putative O_2 concentrations from 1 to
497 10,000 nM during the SR1805 cruise. Experiments were conducted with waters from the ODZ
498 top: 93 – 110m (PS1) (A, D), 113 – 130m (PS2) (B, E), and 45 – 60m (PS3) (C, F). Error bars
499 are the standard error of the regression. All rates were significantly different from zero.

500

501 3.3 NO_2^- dismutation

502

In order to investigate the mechanism for the observed anaerobic NO_2^- oxidation,

503

experiments were conducted to search for evidence of NO_2^- dismutation. If NO_2^- dismutation is

504

the dominant explanation for the observed anaerobic NO_2^- oxidation, we hypothesized that (1)

505

adding NO_3^- should suppress both $^{30}\text{N}_2$ and NO_3^- production by LeChatelier's principle, (2)

506

increasing $^{15}\text{NO}_2^-$ concentration should increase both denitrification (the $^{30}\text{N}_2$ production rate)

507

and NO_2^- oxidation especially when no additional NO_3^- was added, and (3) that the ratio

508

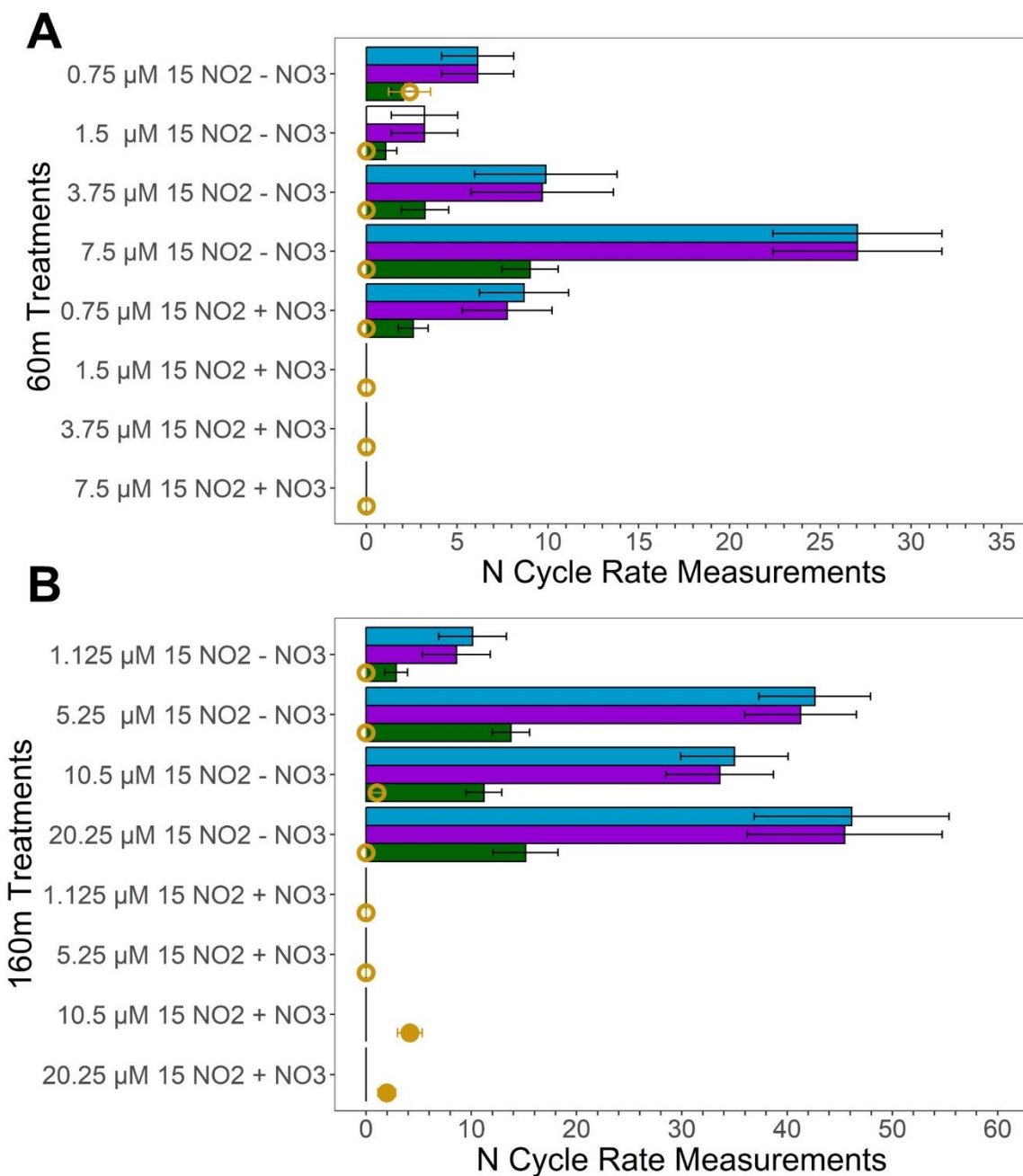
between the “unexplained NO_2^- oxidation,” i.e., the difference between the observed NO_2^-

509

oxidation and the NO_2^- oxidation due to anammox, and the observed denitrification ($^{30}\text{N}_2$

510 production) rate should be close to 3:1. In experiments with He-purged water from two
511 deoxygenated depths (60 and 160 m at station PS3, see table S5 for O₂ values) during the
512 SR1805 cruise we observed that adding 20 μM NO₃⁻ suppressed NO₂⁻ oxidation across nearly all
513 pairs of 0 and 20 μM NO₃⁻ experiments where the NO₂⁻ concentration was identical (Fig. 5).
514 However, we did not observe a simultaneous suppression of N₂ production due to the fact that
515 the measured denitrification rate was low and insignificantly different from zero in most of our
516 16 treatments (Fig. 5). The lack of an observed response in N₂ production could be due to
517 already elevated ambient NO₃⁻ concentrations, 26 μM and 22.2 μM at 60 m and 160 m
518 respectively. Roughly doubling the amount of NO₃⁻ would have little effect on the
519 denitrification rate if the relevant enzymes were already saturated, as is plausible at those
520 concentrations. As a result of our inability to observe denitrification, our first hypothesis yielded
521 little evidence of dismutation.

522 Across all four 60 m 0 μM added NO₃⁻ treatments (Fig. 5A), adding NO₂⁻ did increase
523 NO₂⁻ oxidation; however, we did not observe an increase in denitrification. Surprisingly, across
524 the four 60 m 20 μM added NO₃⁻ treatments, adding NO₂⁻ decreased NO₂⁻ oxidation, the reverse
525 of our hypothesis (Fig. 5). Across all four 160 m 0 μM added NO₃⁻ treatments, we also observed
526 an increase in NO₂⁻ oxidation at higher NO₂⁻ concentrations but did not observe an increase in
527 the measured denitrification rate (Fig. 5B). In the four 160 m 20 μM added NO₃⁻ treatments,
528 NO₂⁻ oxidation and denitrification did not increase with NO₂⁻ concentration (Fig. 5B). Due to
529 the consistently low and insignificant denitrification rates our test of the NO₂⁻ addition
530 hypothesis also yielded little evidence for dismutation.



531

532 **Figure 5:** NO_2^- dismutation tests conducted in deoxygenated waters from 60m (A) and 160m (B)
 533 at station PS3 during the SR1805 cruise. Measured NO_2^- oxidation rates (nM N d^{-1}) are
 534 displayed in blue, unexplained NO_2^- oxidation rates, the difference between the measured NO_2^-
 535 oxidation and the NO_2^- oxidation due to anammox (nM N d^{-1}), are shown in purple. The
 536 predicted denitrification ($\text{nM } ^{30}\text{N}_2 \text{ d}^{-1}$) if all the unexplained NO_2^- oxidation was due to NO_2^-
 537 dismutation is shown in green. The measured denitrification rate ($\text{nM } ^{30}\text{N}_2 \text{ d}^{-1}$) is shown in
 538 yellow where filled circles indicate significant rates and open circles indicate rates that are not
 539 significantly different from zero. All bars filled with colors indicate significant rates (i.e. the
 540 white bar for the 60 m 1.5 μM $^{15}\text{NO}_2^-$, 0 μM NO_3^- treatment NO_2^- oxidation rate denotes an

541 insignificant rate). Error bars are the standard error of the regression for NO_2^- oxidation, or are
542 calculated based on the rules of error propagation from the standard error of the regressions for
543 the NO_2^- oxidation and anammox rates. (+) NO_3^- treatments received $20 \mu\text{M } ^{14}\text{NO}_3^-$ additions
544 while the (-) NO_3^- treatments received no addition. Anammox rates used to calculate the
545 unexplained NO_2^- oxidation rate are shown in the supplementary material.

546
547 We were also unable to observe evidence for the ratio hypothesis due to the paucity of
548 significant denitrification ($^{30}\text{N}_2$ production) rates (Fig. 5). Since denitrification rates were
549 consistently low or insignificantly different from zero, the ratio of NO_2^- oxidation to
550 denitrification deviated from the 3:1 ratio expected if NO_2^- dismutation accounts for most of the
551 observed NO_2^- oxidation. The only slight exception to this is the 60 m treatment with $0.75 \mu\text{M}$
552 $^{15}\text{NO}_2^-$ and $0 \mu\text{M}$ added NO_3^- , the treatment closest to in situ conditions. In this treatment, the
553 measured denitrification rate, while insignificantly different from zero on the basis of the p value
554 of the regression, agrees with the predicted denitrification rate based on the 3:1 stoichiometry of
555 dismutation. While our dismutation experiments as a whole suggest that NO_2^- dismutation is not
556 a likely explanation for observed anaerobic NO_2^- oxidation, results from the 60 m $0.75 \mu\text{M}$
557 $^{15}\text{NO}_2^-$, $0 \mu\text{M}$ NO_3^- treatment provide slight justification to continue tests of this hypothesis.

558

559 4. Discussion

560 4.1 Rapid $\text{NO}_2^- / \text{NO}_3^-$ cycle

561 Depth profiles of N transformation rates obtained on the SR1805 cruise show that the
562 rates of NO_2^- oxidation and NO_3^- reduction are far greater than rates of the N loss processes of
563 anammox and denitrification, especially in shallow boundary (see Table 1 for definition) waters
564 (Fig. 2, Fig. 6A – B). In fact, when the combined N recycling pathways of NO_2^- oxidation and
565 NO_3^- reduction are compared to the total N loss, the N recycling pathways are 3.2 – 192.8 times
566 larger than the total N loss. That the minimum ratio is ~ 3 strongly emphasizes the

567 preponderance of NO_2^- oxidation and NO_3^- reduction above N loss processes. As expected due
568 to the oligotrophic nature of the offshore ETNP (Fuchsman et al., 2019) and as previously found
569 in an ETSP N cycling study (Kalvelage et al., 2013), NO_2^- oxidation and NO_3^- reduction
570 generally increased from the offshore station (PS1) towards the coast. We observed NO_3^-
571 reduction rates of a similar magnitude to previously reported ETSP studies (Kalvelage et al.,
572 2013; Babbin et al., 2017), a finding that generalizes the predominance of NO_3^- reduction to
573 NO_2^- to the ETNP. Thus, our work supports several recent studies (Babbin et al., 2020, 2017;
574 Peters et al., 2016) suggesting that most nitrogen within OMZ regions is continuously recycled
575 between NO_2^- and NO_3^- by rapid NO_2^- oxidation and NO_3^- reduction, especially in shallow
576 boundary waters.

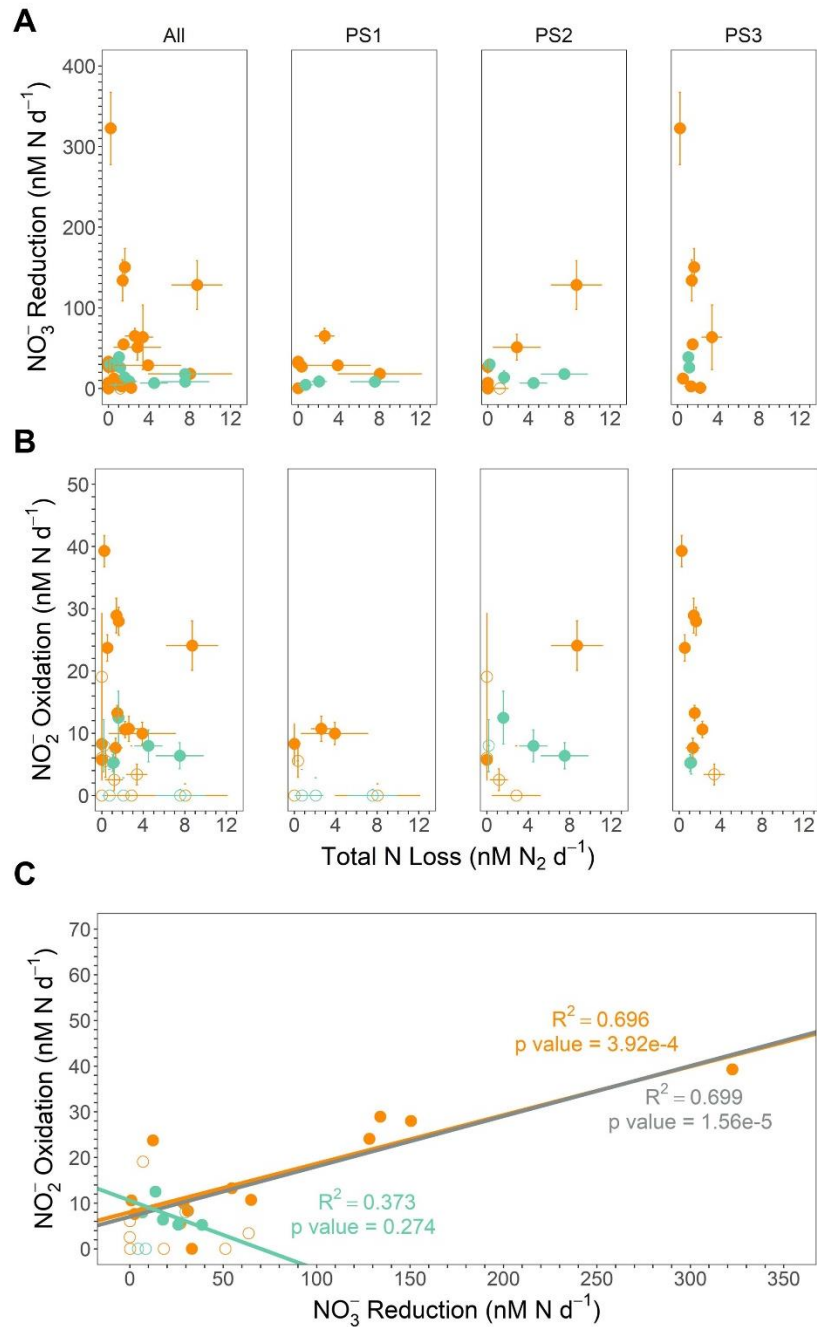
577 A previous work (Babbin et al., 2017) predicted that NO_3^- reduction should follow a
578 Martin curve (Martin et al., 1987) power law distribution across the water column due to its
579 dependence on the OM flux from shallower waters. Such a distribution was observed at stations
580 PS1 and PS3; however, NO_3^- reduction at station PS2 did not follow a classical Martin curve
581 profile since the NO_3^- production peak is well below the oxycline. This exception could be due
582 to zooplankton which have been observed to migrate into the ODZ on a daily basis (Bianchi et
583 al., 2014). Due to the fact that migrating zooplankton funnel surface OM to the mesopelagic
584 (Cram et al., 2022), such a transfer would move OM in a pattern not consistent with the Martin
585 curve. The transferred OM could then support the observed peak in NO_3^- reduction (Fig. 2).

586 These results are consistent with the idea, also supported by many recent studies
587 (Kalvelage et al., 2013; Lam and Kuypers, 2011; Lam et al., 2009; Babbin et al., 2020, 2017;
588 Füssel et al., 2011; Lam et al., 2011), that the accumulated NO_2^- in the SNM usually results from
589 an imbalance between NO_3^- reduction and other N cycling pathways. We further investigated

590 this hypothesis by constructing a net NO_2^- budget derived from the five microbial N cycling
591 metabolisms measured on the SR1805 cruise (Fig. 7). Summing the depth profiles of NO_2^-
592 consumption (anammox, denitrification, and NO_2^- oxidation) and production (NH_4^+ oxidation
593 and NO_3^- reduction) pathways revealed that net depth integrated NO_2^- production across the
594 sampled OMZ water column depths is on the order of tens of millimoles of NO_2^- per square
595 meter per day at all three stations (8.19 at PS1, 14.49 at PS2, and 28.97 $\text{mmol NO}_2^- \text{ m}^{-2} \text{ d}^{-1}$ at
596 PS3). This excess NO_2^- is driven by NO_3^- reduction, which across all stations is of a much
597 greater magnitude than all other measured N cycling processes (Fig. 2 and Fig. 7).

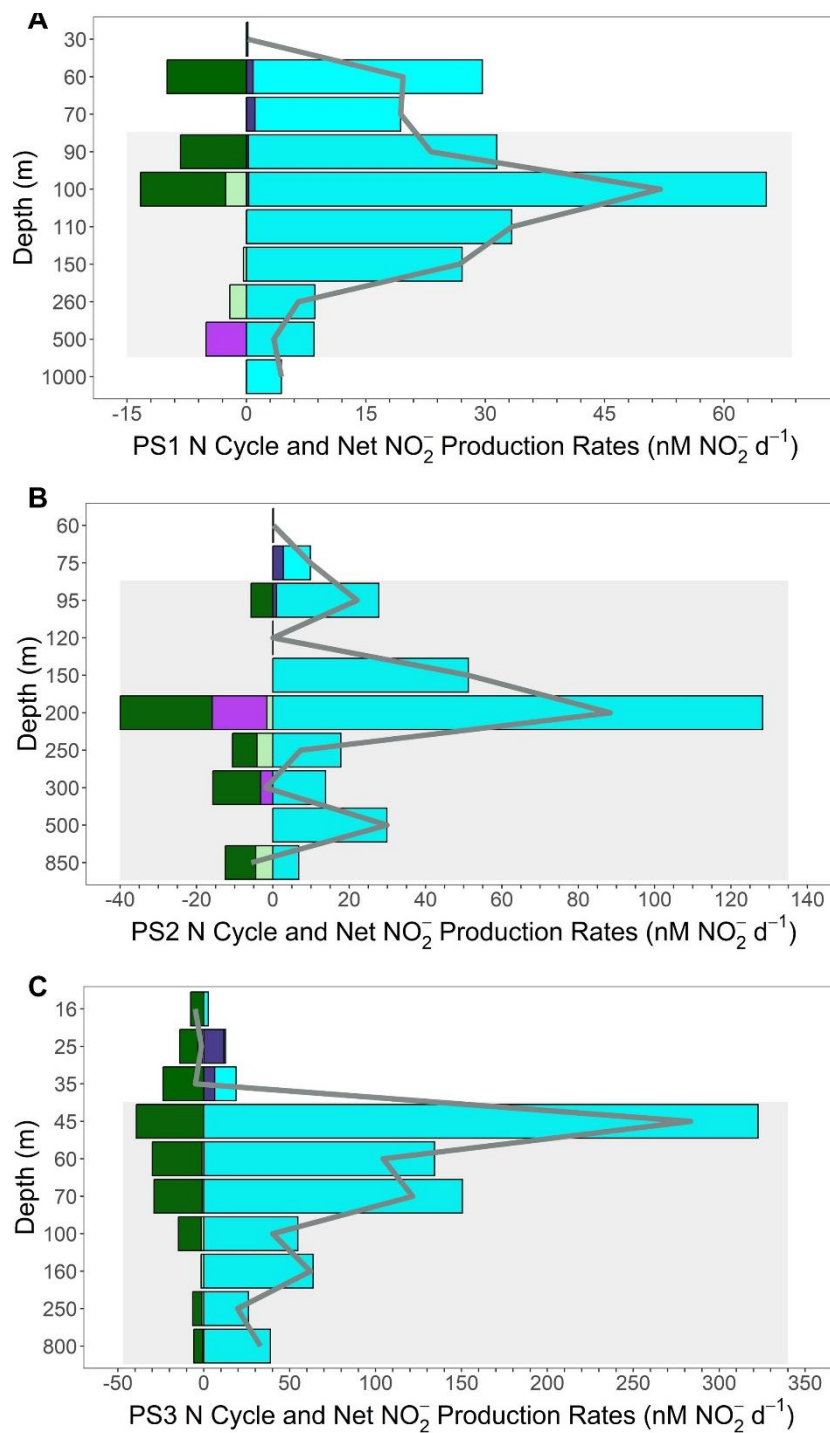
598 These budget calculations take the reported rates at face value, ignoring the likelihood
599 that some of them are potential rates. For example, anammox might have been enhanced by the
600 addition of 3 $\mu\text{M NH}_4^+$. Denitrification is less likely to be stimulated by the addition of NO_2^- ,
601 because it is generally limited by organic matter availability (Ward et al. 2008, Babbin et al
602 2014). Thus, the relative importance of anammox and denitrification might be perturbed due to
603 differential responses of the two rates to tracer additions. Analogously, NO_2^- oxidation was
604 likely stimulated by addition of NO_2^- tracer (Sun et al. 2017), but NO_3^- reduction less so by
605 addition of NO_3^- tracer because the latter is a heterotrophic process, and as a component of the
606 complete denitrification pathway, likely limited by organic matter availability. These differential
607 limitations by substrate probably mean that the calculated budget of Figure 7 is not completely
608 accurate, but the relative importance of the processes is robust. If anything, the dominance of
609 anammox over denitrification is probably less than that observed, and the excess of NO_3^-
610 reduction over NO_2^- oxidation greater than observed. Overall, the dominance of the $\text{NO}_3^- / \text{NO}_2^-$
611 loop over the N loss pathways and the overwhelming importance of NO_3^- reduction are both
612 supported by these considerations.

613 Additional support that NO_3^- reduction supplies the accumulated NO_2^- in the SNM can
614 be found by comparing the net NO_2^- production rates with the measured NO_2^- concentrations
615 along the SR1805 cruise track from offshore station PS1 to coastal station PS3. As would be
616 expected if the SNM depended on NO_2^- derived from NO_3^- reduction, the peak net NO_2^-
617 production value across all depths at each station, the depth integrated NO_2^- production values
618 for each station, and the magnitude of the SNM peak NO_2^- concentrations all increase together
619 from offshore station PS1 to coastal station PS3. Importantly, we did not take into account water
620 column mixing in both vertical and horizontal directions that would carry away produced NO_2^-
621 or NO_2^- assimilation into OM, and we recommend follow up studies that include
622 parameterizations for these values in OMZ N Cycling modeling.



623

624 **Figure 6:** (A) NO_3^- reduction (nM N d^{-1}) vs. Total N loss (the sum of denitrification and
 625 anammox in $\text{nM N}_2 \text{d}^{-1}$) from the SR1805 cruise. (B) NO_2^- oxidation (nM N d^{-1}) vs. Total N loss
 626 from the SR1805 cruise. (C) NO_2^- oxidation vs. NO_3^- reduction. Regression lines and statistics
 627 are shown for the significant rates from shallow boundary waters only (orange), ODZ core
 628 waters only (teal), and all significant data (grey). All points from shallow boundary waters are
 629 colored orange while all points from the ODZ core or below are colored teal. Open circles
 630 indicate points where the NO_3^- reduction rate (A), NO_2^- oxidation rate (B), or in (C) either NO_3^-
 631 reduction or NO_2^- oxidation rate is not significantly different from zero while filled circles
 632 indicates rates significantly different from zero.

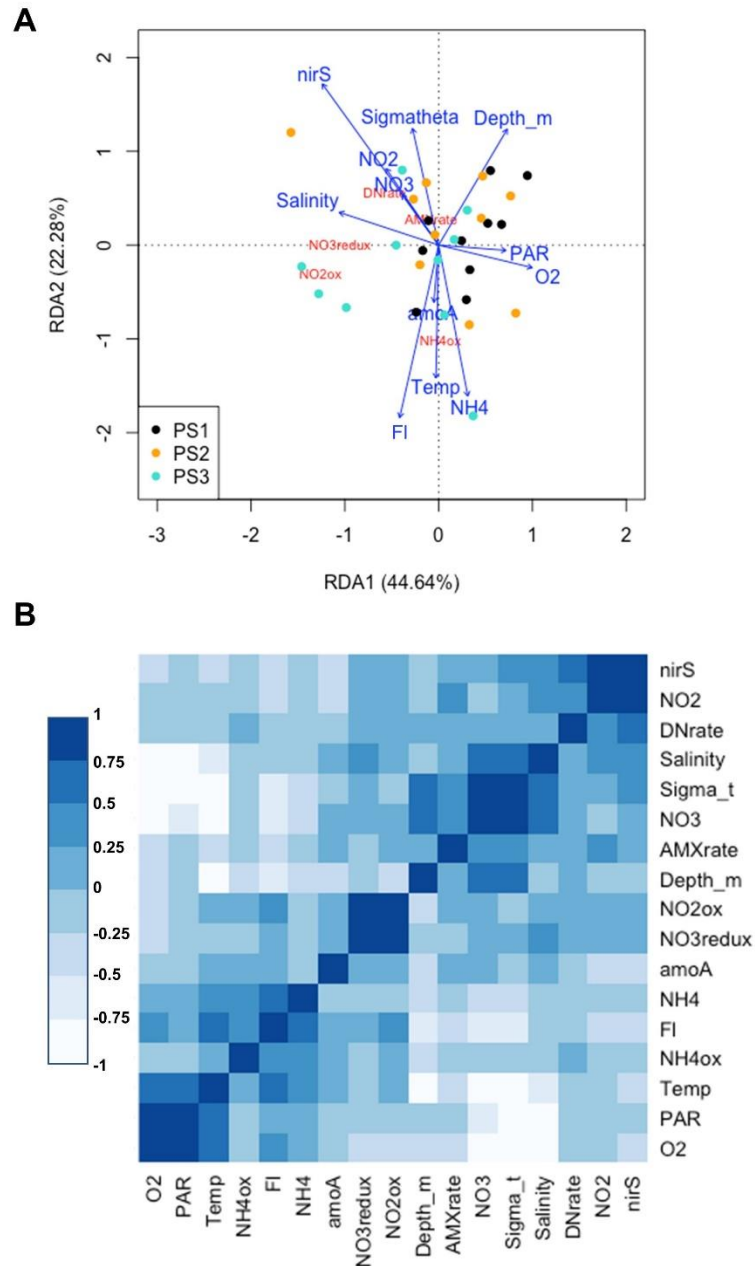


633
634

635 **Figure 7:** NO_2^- budget profiles from the SR1805 cruise. Plots are a combination of the NO_2^-
636 production pathways of NO_3^- reduction (cyan), NH_4^+ oxidation (dark purple) and the NO_2^-
637 consumption pathways of anammox (light green), denitrification (bright purple), and NO_2^-
638 oxidation (dark green). Consumption pathways are reported as negative numbers. All rates are
639 reported in $\text{nM NO}_2^- \text{d}^{-1}$. The net NO_2^- production or consumption rate ($\text{nM NO}_2^- \text{d}^{-1}$) is
640 represented as a grey line for each depth. Grey boxes indicate the completely deoxygenated
641 ODZ region at each station at the time of sampling. (A) PS1, (B) PS2, and (C) PS3.

642 4.2 NO₂⁻ oxidation – distribution and magnitude in comparison to previous studies

643 The high rates of observed NO₃⁻ reduction provide sufficient NO₂⁻ to support NO₂⁻
644 oxidation both in the oxycline and in the ODZ, as previously proposed (Anderson et al., 1982),
645 Our observations also further confirm isotopic studies that suggested high NO₂⁻ oxidation rates
646 because rapid re-oxidation of NO₂⁻ back to NO₃⁻ was necessary to achieve isotopic mass balance
647 (Buchwald et al., 2015; Casciotti et al., 2013; Granger and Wankel, 2016). Our results also align
648 with previous experimental observations of high NO₂⁻ oxidation rates (Kalvelage et al., 2013;
649 Babbin et al., 2020; Lipschultz et al., 1990). Support for a closely connected rapid cycle
650 between the two processes can be seen in the strong correlation between NO₂⁻ oxidation and
651 NO₃⁻ reduction observed in all SR1805 cruise samples, especially those from shallow boundary
652 waters (Fig. 6C, Fig. 8). Similarly to some previous ETSP papers (Babbin et al., 2017, 2020;
653 Frey et al., 2020) and two ETNP studies (Peng et al., 2015; Sun et al., 2017) we observed that
654 rates of NO₂⁻ oxidation, like rates of NO₃⁻ reduction, peaked in the oxycline or in the ODZ top
655 (Fig. 2) and then declined throughout the ODZ. Unlike some stations in these studies (Babbin et
656 al., 2020, 2017) we did not observe a second peak in NO₂⁻ oxidation near the deep oxycline. In
657 addition to observing a similar distribution, we also observed that NO₂⁻ oxidation occurs at a
658 similar magnitude to some stations in previous ETSP studies (Babbin et al., 2020, 2017; Peng et
659 al., 2016) and ETNP (Peng et al., 2015), although our highest rates (25 – 40 nM N d⁻¹) were
660 much lower than the peaks measured at other stations in most of these reports (Babbin et al.,
661 2020; Peng et al., 2015, 2016), which reached as high as ~600 nM N d⁻¹ (Peng et al., 2015;
662 Lipschultz et al., 1990).



663

664 **Figure 8:** (A) Redundancy analysis of all environmental variables and microbial rates measured
 665 on the SR1805 cruise. Points are color-coded by station, black (PS1), yellow (PS2), and cyan
 666 (PS3). Variables names and arrows are color coded so that environmental variables are blue and
 667 rate measurements are red. (B) Correlation analysis for all environmental variables and
 668 microbial N cycle rates from the SR1805 cruise. More positive correlations are shaded to
 669 become bluer as significance grows while negative correlations are shaded to become whiter as
 670 significance grows. Abbreviations used are as follows: O2 (oxygen concentration normalized
 671 across different sensors), PAR (photosynthetically active radiation normalized across sensors),
 672 NH4ox (NH₄⁺ oxidation rate), FI (chlorophyll fluorescense normalized across different sensors),
 673 NH4 (NH₄⁺ concentration), *amoA* (*amoA* abundance), NO₃⁻redux (NO₃⁻ reduction rate), NO₂ox

674 (NO_2^- oxidation rate), AMXrate (anammox rate), NO_3^- (NO_3^- concentration), DNrate
675 (denitrification rate), NO_2 (NO_2^- concentration), and *nirS* (*nirS* abundance).

676

677

678 **4.3 NO_2^- oxidation – can it occur anaerobically?**

679 NO_2^- oxidation depth profiles (Figs. 2, 3) and O_2 manipulation experiments (Fig. 4)

680 provide further evidence that NO_2^- oxidation can occur even when O_2 is as low as ~ 1 nM. .

681 While our O_2 manipulation experiments provide the most convincing evidence of anaerobic

682 NO_2^- oxidation, several factors argue that the NO_2^- oxidation observed in our depth profile

683 incubations may be O_2 independent. As argued previously (Babbin et al., 2020):

684 (1) The pre-incubation He purging step in our depth profile method removes more than 99% of

685 the N_2 present in exetainers (Babbin et al., 2020). If it is assumed that O_2 is removed at identical

686 efficiency, a reasonable proposition since O_2 equilibrates faster than N_2 (Wanninkhof, 1992), the

687 introduction during sample processing of as much as $1 \mu\text{M}$ O_2 would result in a ~ 10 nM

688 contamination. As a result, if NO_2^- oxidation is observed in samples from the deoxygenated ODZ

689 core, contamination during sampling would be kept very small by our purging step. This

690 conclusion was further validated by direct O_2 measurements using Lumos sensors in exetainers.

691 These tests of our purging method showed that O_2 was reduced to less than 10 nM in 5 minutes

692 (Sun et al. unpublished data).

693 (2) Linear timecourses across all timepoints were observed in some of our experiments,

694 including many from deoxygenated depths at station PS3 (Supplemental Figs. S7-9). If NO_2^-

695 oxidation depended on O_2 , an initial acceleration (due to O_2 contamination that sparked NO_2^-

696 oxidation) or later steep drop (due to the exhaustion of O_2 by aerobic NOB) in NO_2^- oxidation

697 would be expected, not a consistent linear slope.

698 (3) Metagenomic evidence has revealed distinct NOB communities in oxic surface waters, the
699 oxycline and ODZ top, and the ODZ core in OMZ regions (Sun et al., 2019). In addition we
700 observed decreasing NO_2^- oxidation rates with increasing in situ O_2 in the SR1805 incubations as
701 well as the TN278 and NBP1305 incubations (Fig. 3A). These observations are consistent with
702 the hypothesis that aerobic NOB from oxic depths are ill-equipped to oxidize NO_2^- in
703 deoxygenated conditions but that the unique MAGs recently identified in draft genomes from the
704 ODZ top and core (Sun et al., 2019), are adapted to perform anaerobic NO_2^- oxidation.

705 (4) Through plotting O_2 concentrations against the ratio between NO_3^- reduction and NO_2^-
706 oxidation at all SR1805 depths with significant, positive NO_2^- oxidation rates, we observed that
707 the known anaerobic process of NO_3^- reduction and NO_2^- oxidation did not exhibit differential
708 regulation by O_2 as would be expected if NO_2^- oxidation was an obligately aerobic process (Fig.
709 S5).

710 Previous studies have shown that O_2 additions to purged incubations of ODZ waters can
711 inhibit NO_2^- oxidation (Sun et al., 2017, 2021a) and that NO_2^- oxidation can occur in the absence
712 of O_2 consumption (Sun et al., 2021a). However, another kinetics study has reported O_2
713 stimulation of NO_2^- oxidation in OMZ waters (Bristow et al., 2016) and concluded that NO_2^-
714 oxidation is fundamentally an aerobic process. This apparent contradiction might be explained
715 by several details in the experimental process of that study (Bristow et al., 2016):

716 (1) The study site is at the farthest edge of the ETSP OMZ in a location that is only anoxic in the
717 austral summer.

718 (2) The cruise was conducted as austral summer turned to fall (March 20 – 26th), a period where
719 O_2 intrusions would be more likely.

720 (3) O₂ data from the study's cruise (Tiano et al., 2014) show that the depths from which NO₂⁻
721 oxidation O₂ kinetics samples were sourced experienced O₂ concentrations of 2 μM (50 m), 10
722 μM (40 m), and > 60 μM (30m) either during sampling or a few days prior to sampling.
723 As a result, we argue that the observed stimulation of NO₂⁻ oxidation by O₂ (Bristow et al., 2016)
724 occurred not because all OMZ NOB are aerobic NO₂⁻ oxidizers, but instead because the location,
725 season, and levels of O₂ of the sampled station selected for aerobic NOB in the source water for
726 the purged incubations. Thus, as suggested by (Sun et al., 2017, 2021a), different NOB
727 populations with different historical exposures to O₂ and adaptations likely respond differently to
728 O₂ manipulations.

729 Here we built on the above previous tests of anaerobic NO₂⁻ oxidation by conducting a
730 series of incubations across an O₂ gradient from ~1 nM to 10 μM. Site waters for these
731 incubations were drawn from the ODZ top at each SR1805 station (Table S4). We did not
732 observe a clear inhibitory or stimulatory response of NO₂⁻ oxidation to O₂ within the SR1805 or
733 FK180624 stations; however, this lack of a clear response is in itself a revealing result - a lack of
734 consistent stimulation by O₂ implies at least some anaerobic NOB were present. In addition, we
735 consistently observed significant NO₂⁻ oxidation at all putative O₂ concentrations, including 1
736 nM, a concentration usually considered functionally anoxic. Since the O₂ in the incubations was
737 continuously supplied by a mass flow controller and subsequently checked via an extremely
738 sensitive O₂ sensor for all incubations, these results provide additional evidence that truly
739 anaerobic NO₂⁻ oxidation can occur.

740 One argument against our characterization of the NO₂⁻ oxidation observed at ~1 nM O₂
741 as functionally anoxic is that the K_m of NO₂⁻ oxidation has been calculated to be as low as 0.5
742 nM (Bristow et al., 2016). However, the data used to calculate this value have the same

743 qualifications discussed previously: (1) the study site is at a location only anoxic during the
744 austral summer, (2) the cruise was conducted during a time when O₂ intrusions would be more
745 likely, and (3) the sampled waters experienced O₂ concentrations as high as 60 μM prior to
746 sampling. Such conditions would favor aerobic NOB and the expression of high affinity NO₂⁻
747 oxidation enzymes by these organisms when exposed to low O₂ conditions in incubations. As a
748 result, we argue that the modeled K_m value of 0.5 nM only applies when NOB with higher O₂
749 niches are placed in sub-micromolar O₂ conditions. This value does not apply to NOB observed
750 to prefer ODZ conditions (Sun et al., 2019), which we assume would be favored under our 1 nM
751 treatment.

752 These O₂ manipulation experiments also provided an opportunity to investigate the
753 response of NO₃⁻ reduction to O₂. The only clear intra-station pattern that emerged from these
754 experiments was that at station PS3, NO₃⁻ reduction displayed possible inhibition by O₂, as
755 would be expected. Due to the small number of data points in our data set we did not attempt a
756 kinetics fitting for this data. Interestingly, the disparity observed in depth profile experiments
757 between the magnitudes of the NO₃⁻ reduction and NO₂⁻ oxidation rates was not observed in the
758 O₂ manipulations across many O₂ concentrations at stations PS1 and PS2. At station PS3 a large
759 disparity in the magnitudes of these processes as well as the highest overall NO₃⁻ reduction rates
760 were observed, as in the depth profile experiments (Fig. 4, 7). A few of the FK180624 data
761 points also exhibited NO₃⁻ reduction rates that were elevated far above NO₂⁻ oxidation (Fig. S3).
762 These results confirm the importance of NO₃⁻ reduction for the rapid recycling cycle as well as
763 the source of NO₂⁻ for the SNM.

764

765 **4.4 NO₂⁻ dismutation**

766 In the absence of O₂, NO₂⁻ oxidation would require another oxidant. Many candidate
767 oxidants have been suggested. For example, iodate (IO₃⁻), an abundant marine species with
768 global average marine concentrations of ~0.5 μM (Nozaki, 1997; Lam and Kuypers, 2011), has
769 been proposed and shown to stimulate NO₂⁻ oxidation (Babbin et al., 2017). However, since
770 IO₃⁻ is usually absent within the ODZ core (Moriyasu et al., 2020), its low concentration makes
771 IO₃⁻ mediated anaerobic NO₂⁻ oxidation in that location unlikely (Babbin et al., 2020). NO₂⁻
772 oxidation via Mn⁴⁺ or Fe³⁺ is thermodynamically feasible, but only at low pH (<6) (Luther, 2010;
773 Luther and Popp, 2002). This pH constraint, combined with the fact that concentrations of these
774 ions are on the order of a few nM in OMZs (Kondo and Moffett, 2015; Vedamati et al., 2015),
775 makes these mechanisms unrealistic for the ODZ core. Another proposed mechanism is that the
776 observed NO₂⁻ oxidation is due to anammox, which if true should result in an observed NO₂⁻
777 oxidation to anammox ratio of 0.16 – 0.3 (Kuenen, 2008; Strous et al., 1998; Oshiki et al., 2016).
778 Instead, the observed ratio is sometimes more than 10x this range and NO₂⁻ oxidation is rarely
779 observed to be less than anammox (Kalvelage et al., 2013; Babbin et al., 2020; Sun et al., 2021a).

780 Another alternative hypothesis is based on the reversibility of the nitrite oxidoreductase
781 (NXR) enzyme. Since this enzyme has been suggested to both oxidize NO₂⁻ and reduce NO₃⁻
782 (Kemeny et al., 2016; Koch et al., 2015; Wunderlich et al., 2013), NO₃⁻ reduction by NXR could
783 over time enrich the ¹⁵N-NO₃⁻ pool since lighter ¹⁴N-NO₃⁻ would be favored (Casciotti, 2009).
784 Even in ¹⁵NO₂⁻ tracer experiments, in which the NO₂⁻ pool is highly labeled, this reversibility at
785 the enzyme site could lead to an apparent transfer of ¹⁵N from the NO₂⁻ to the NO₃⁻ pool if NXR
786 mediated NO₃⁻ reduction was occurring. This hypothesis is supported by observations of NO₃⁻
787 reduction under low O₂ in cultures from the NOB genera *Nitrobacter* (Freitag et al., 1987; Bock
788 et al., 1990), *Nitrospira* (Koch et al., 2015), and in pure cultures of *Nitrococcus mobilis* (Füssel

789 et al., 2017). In addition, a recent study presented natural abundance isotopic evidence in pure
790 *Nitrococcus mobilis* cultures consistent with this mechanism (Buchwald and Wankel, 2022).

791 However, NXR reversibility has not been demonstrated for the abundant (Füssel et al.,
792 2011; Mincer et al., 2007) and sometimes dominant (Beman et al., 2013) OMZ NOB genera
793 *Nitrospina*. Furthermore, the sole source of the isotopic evidence for the enzyme reversibility
794 hypothesis, *Nitrococcus mobilis*, has a cytoplasm facing NXR substrate binding domain
795 (Buchwald and Wankel, 2022), a feature found to have an established evolutionary relationship
796 to NAR (the known NO_3^- reductase enzyme family) in other *Nitrobacter* studies (Starkenburg et
797 al., 2008; Kirstein and Bock, 1993). The NXR substrate binding domains in *Nitrospina* are
798 oriented towards the periplasm and are not evolutionarily related to enzymes for NO_3^- reduction
799 (Buchwald and Wankel, 2022; Sun et al., 2019). Due to these structural and phylogenetic
800 differences among NOB NXR, it is possible that the *Nitrospina* NXR may be unable to perform
801 NO_3^- reduction as easily as other NOB genera. For all these reasons, it is not yet clear if the
802 enzyme reversibility hypothesis can explain all NO_2^- oxidation measured under low O_2
803 conditions and other hypotheses should continue to be explored.

804 As a result of the above proposals' shortcomings, this paper focused on the remaining,
805 most plausible hypothesis: NO_2^- dismutation. Our tests for dismutation rested on three
806 hypotheses: (1) that NO_3^- additions would inhibit both NO_2^- oxidation and $^{30}\text{N}_2$ production by
807 LeChatelier's principle, (2) that increasing $^{15}\text{NO}_2^-$ should energetically favor dismutation,
808 especially in treatments with no additional NO_3^- , and (3) that the ratio of non-anammox
809 mediated NO_2^- oxidation to denitrification ($^{30}\text{N}_2$ production) should be close to 3:1 if NO_2^-
810 dismutation explains most of the observed NO_2^- oxidation. We observed repeated inhibition of
811 NO_2^- oxidation by NO_3^- but no inhibition of $^{30}\text{N}_2$ production due to the fact that denitrification

812 was consistently low and insignificantly different from zero across all treatments. In treatments
813 with 0 μM added NO_3^- , increasing NO_2^- generally increased NO_2^- oxidation, but not
814 denitrification. In addition, the ratio of anammox corrected NO_2^- oxidation to observed
815 denitrification deviated from dismutation's 3:1 stoichiometry in almost all treatments. However,
816 we did observe simultaneous inhibition of N_2 and NO_3^- production as well as good agreement
817 between the anammox corrected NO_2^- oxidation / denitrification ratio to the NO_2^- dismutation
818 stoichiometry in one treatment - the treatment most similar to in situ conditions (60m, 0.75 μM
819 $^{15}\text{NO}_2^-$, 0 μM NO_3^-). As a result, while our results show little evidence for dismutation overall,
820 we recommend additional experiments at tracer levels similar to 0.75 μM $^{15}\text{NO}_2^-$ to further test
821 for NO_2^- dismutation.

822

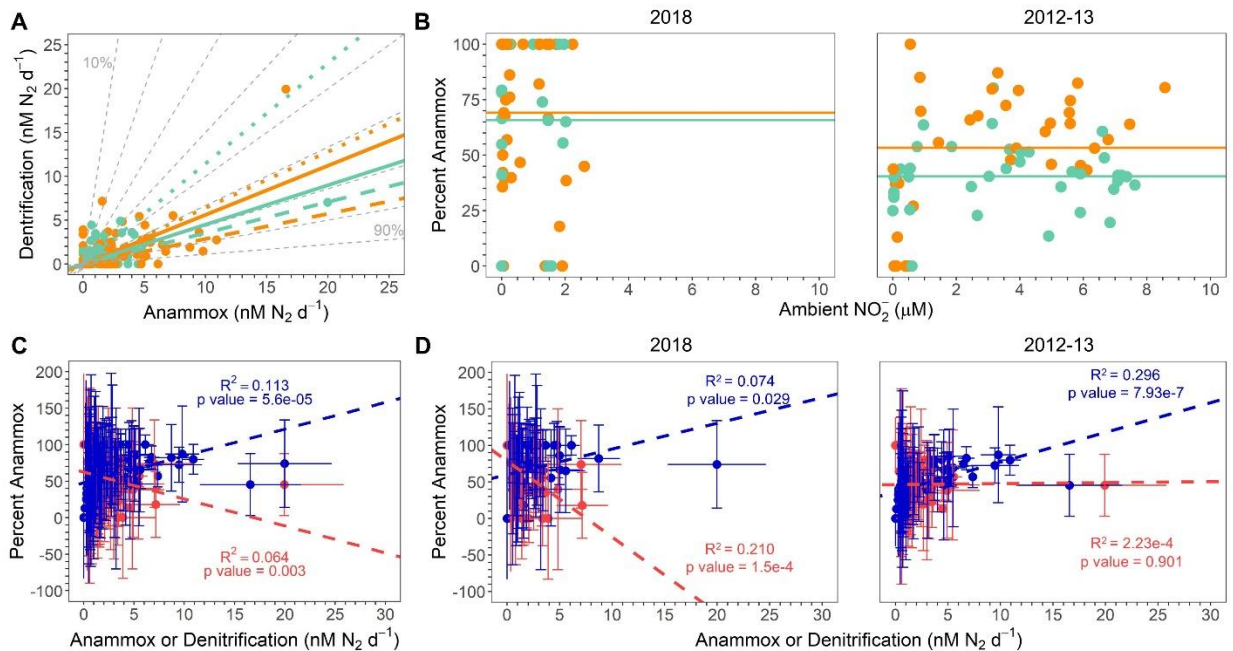
823 **4.5 Relative balance of anammox and denitrification**

824 **4.5.1 Are results consistent with past observations of slow, low, and steady anammox** 825 **elevated above the predicted maximum of 29% of total N loss?**

826 According to predictions based on the composition of average marine OM (Dalsgaard et
827 al., 2003, 2012) anammox should account for at most 29% of the total N loss flux in OMZ
828 regions. To test this hypothesis under a variety of conditions, regressions of denitrification vs.
829 anammox rates were calculated for all samples from the SR1805, FK180624, TN278, and
830 NBP1305 cruises. In order to compare our new data to a previous study (Babbin et al., 2020),
831 which observed variations in the ratio of anammox and denitrification between samples from the
832 ODZ top or above ($\sigma_\theta < 26.4$, "shallow boundary waters," (Babbin et al., 2020)) and samples
833 from the deoxygenated ODZ core or below ($\sigma_\theta > 26.4$, "ODZ core," (Babbin et al., 2020)),
834 regressions for all data (ODZ core), all data (shallow boundary), 2018 only (ODZ core), 2018

835 only (shallow boundary), 2012-13 (TN278, and NBP1305) only (ODZ core), and 2012-13 only
836 (shallow boundary) were calculated (Table S6). All regressions deviated from the predicted 29%
837 maximum anammox contour, although the regression from the 2012-13 cruises' ODZ core
838 samples was closest to the 30% anammox contour (Fig. 9A). We observed large differences in
839 the percent anammox contours near 2012-13 and 2018 regressions. ODZ core samples from
840 2012-13 regressed onto a line between the 40 and 50% anammox contours while ODZ core
841 samples from 2018 regressed onto a line between the 70% and 80% anammox contours.
842 Differences in contouring were smaller for the shallow boundary samples, although the 2018
843 samples still regressed to a higher contour (just under 80%) than the 2013-13 samples (60%)
844 (Fig. 9A). Our observations that all year and density based regressions fell within contours well
845 above the theoretical prediction (Fig. 9A) and that anammox accounted for as much as 100% of
846 the total N loss at many depths in 2018 samples (Fig. 2, Fig. 9B) is consistent with the many
847 previous studies that observed anammox as the predominant OMZ N loss pathway (Lam et al.,
848 2009; Thamdrup et al., 2006; Kuypers et al., 2005; Hamersley et al., 2007; Jensen et al., 2011).

849 Our new 2018 results do not contradict the idea (Dalsgaard et al., 2012) that anammox is
850 often measured to be the bulk of total N loss but that large, episodic occurrences of denitrification
851 can dwarf the consistent albeit low anammox contribution to total N loss. Under this view, these
852 eruptions in denitrification return the *time integrated* balance of anammox and denitrification to
853 its expected 29 and 71% values. In this scenario, our cruises' sampling, like many but not all
854 others, did not coincide with episodic high rates of denitrification.



855

856 **Figure 9:** (A) All 2012, 2013, and 2018 denitrification and anammox rates ($\text{nM N}_2 \text{d}^{-1}$), color-
 857 coded by σ_θ . ODZ core samples and lines are teal ($\sigma_\theta > 26.4$) while shallow boundary samples
 858 and lines are orange ($\sigma_\theta < 26.4$). Solid, dashed, and dotted lines respectively show regressions
 859 for all data, 2018 only, and 2012-13 data only. Dashed grey lines depict contours for percent
 860 anammox values. See Supplementary Table S6 for regression statistics. (B) Percent anammox
 861 vs. ambient NO_2^- for 2018 samples (left) and republished 2012 and 2013 samples (Babbin et al.,
 862 2020) (right). Points are colored according to the same scheme as panel A. Lines show the
 863 average percent anammox values in shallow boundary waters (orange) and the deoxygenated
 864 ODZ core (teal). (C) Percent anammox vs. all anammox (blue) and all denitrification (red)
 865 rates ($\text{nM N}_2 \text{d}^{-1}$). Regression lines shown for % AMX vs. anammox and denitrification rates follow
 866 the same color scheme as the data points. Error bars represent the standard error of the
 867 regression. (D) Percent anammox vs. anammox (blue) and denitrification (red) rates ($\text{nM N}_2 \text{d}^{-1}$)
 868 for 2018 only (left) and 2012-13 (right). Points and regression lines follow the same color
 869 scheme as in panel C. Data shown in the 2012-13 only panel are republished (Babbin et al.,
 870 2020).

871

872

873 4.5.2 Do results support a connection between rapid NO_3^- reduction and elevated

874 anammox?

875 Our 2018 results question the previously proposed view (Babbin et al., 2020) that rapid

876 NO_3^- reduction produces NH_4^+ that in turn elevates anammox in oxycline and upper ODZ

877 waters. While our data (Fig. 2) did find high rates of NO_3^- reduction in shallow boundary

878 waters, the 2018 N loss data do not show elevated shallow boundary (as compared to ODZ core)
879 percent anammox values as would be expected if high NO_3^- reduction were fueling elevated
880 anammox in the oxycline and ODZ top. This difference between our 2018 data and some
881 previous data (Babbin et al., 2020) in support of a connection between rapid NO_3^- reduction and
882 elevated anammox in the oxycline and ODZ top can be seen through a comparison of shallow
883 boundary ($\sigma_\theta < 26.4$ (Babbin et al., 2020)) and ODZ core ($\sigma_\theta > 26.4$ (Babbin et al., 2020)) percent
884 anammox values in the 2018 SR1805 and FK180624 cruises against the 2012-13 TN278 and
885 NBP1305 cruises (Fig. 9B). 2012-13 samples showed a clear partitioning between the ODZ core
886 and shallow boundary waters in terms of percent anammox values. In 2012-13, as would be
887 expected if high oxycline and ODZ top NO_3^- reduction were supplying NH_4^+ to anammox,
888 shallow boundary samples have a higher average percent anammox value than ODZ core
889 samples (Fig. 9B). In 2018, this partitioning was not present - the difference between the
890 average percent anammox values in ODZ core and shallow boundary samples was much smaller
891 (Fig. 9B). Interestingly, the total number of samples found to be 100% anammox also sharply
892 diverged between 2012-13 and 2018. In the 2012-13 samples, only one shallow boundary
893 sample was found to be 100% anammox. In 2018, many samples from both shallow boundary
894 waters and the ODZ core were 100% anammox (Fig. 9B, Fig. S6).

895 These observed differences in the partitioning of anammox and denitrification between
896 shallow boundary waters and the ODZ core across different years and places do not support the
897 view that NH_4^+ from rapid NO_3^- reduction of oxycline and ODZ top OM always elevates
898 anammox rates. Instead, they suggest that other factors play an important role in setting the
899 balance of anammox and denitrification. Interestingly, NO_2^- concentrations spanned a much
900 narrower range in the two 2018 SR1805 and FK180624 cruises than the 2012-13 TN278 and

901 NBP1305 cruises (Fig. 9B), a clue that the biogeochemical environment of the OMZ is subject to
902 interannual variability. Observed differences in environmental variables like NO_2^- and percent
903 anammox partitioning between 2012, 2013, and 2018 suggest that the partitioning of total N loss
904 must depend on additional yet to be identified environmental or biological interactions.

905

906 **4.5.3 Correlations of percent anammox values to anammox and denitrification rates -** 907 **comparison to previous literature**

908 In order to re-examine the result (Babbin et al., 2020) that enhanced fractions of
909 anammox are correlated to greater anammox rates and not lower denitrification (Fig. 9D right),
910 we created percent anammox vs. anammox and denitrification regressions with the 2018 SR1805
911 and FK180624 data. In 2018, unlike in 2012-13 (Babbin et al., 2020), we observed significant
912 relationships between percent anammox values and both the anammox and denitrification rates
913 (Fig. 9D left). Regressions for the 2012-13 data showed that increases in % anammox values are
914 correlated only to increases in anammox values, not decreases in denitrification (Babbin et al.,
915 2020) (Fig. 9D right). The 2018 regressions, on the other hand, indicate that increases in %
916 anammox are correlated with both increasing anammox and decreasing denitrification rates. The
917 influence of this difference in the 2018 samples can be seen in regressions of % anammox
918 against anammox and denitrification from all three cruises where a similar pattern to the 2018
919 data is observed (Fig. 9C). As above, this indicates a clear difference in the partitioning of
920 anammox and denitrification between the 2018 SR1805 and FK180624 ETNP cruises and the
921 2012-13 TN278 and NBP1305 cruises to the ETNP and ETSP. Despite the significance of the
922 relationships, the low R^2 values indicate that these relationships do not explain most of the

923 variation in the anammox to denitrification ratio. As above, the causal mechanisms behind this
924 variability remains to be elucidated.

925

926 **4.5.4 Caveats about measurements of anammox and denitrification rates**

927 One bias of our sampling scheme for N loss rates is that we do not capture particle
928 adhering denitrifiers. Most denitrifiers that encode the last two steps of denitrification are found
929 on large particles (Ganesh et al., 2013, 2015; Fuchsman et al., 2017). As a result, measurements
930 of complete denitrification from $^{15}\text{NO}_2^-$ to $^{30}\text{N}_2$ that do not capture large particle communities
931 will underestimate the rate. Unfortunately, due to the hydrodynamics of the CTD rosette it is
932 unlikely that large particles will be trapped inside the Niskin bottle. In addition, the nipple of
933 each Niskin is above the bottom of the bottle. As a result, the large particles that are successfully
934 sampled by the CTD sink to the bottom of the Niskin and are not transferred into the experiment
935 (Suter et al., 2017).

936 Another important caveat to some of the above conclusions in section 4.5 is that the
937 detection limits for anammox and denitrification rates are not identical. It is easier to detect
938 anammox for a variety of reasons. For example, anammox from a $^{15}\text{NH}_4^+$ tracer is more easily
939 detected due to low background NH_4^+ across most of the OMZ. Anammox from the $^{15}\text{NO}_2^-$
940 tracer is more detectible due to its reliance on incorporation of only a single ^{15}N atom into the
941 $^{29}\text{N}_2$ product. Denitrification, on the other hand, is more difficult to detect because of higher
942 background NO_2^- concentrations and because definitive denitrification requires the rarer
943 combination of two $^{15}\text{NO}_2^-$ molecules (Babbin et al., 2017).

944 We suspect that our sampling bias against particle based denitrification and
945 denitrification's higher detection limit may have played a role in our observations of

946 denitrification rates in the 2012, 2013, and 2018 cruises where, for example, significant
947 denitrification rates were only detected at four of the thirty depths sampled during SR1805
948 (Supplementary Table S3). As a result, while the comparisons made above are helpful to
949 examine differences in N biogeochemistry across years and stations, the true biogeochemical
950 role of denitrification is likely greater than our tracer experiments suggest.

951 An additional important consideration is the possibility that anammox was stimulated by
952 our tracer additions, which substantially enriched the NO_2^- and especially the NH_4^+
953 concentrations above their in situ values (see Table S7 for enrichment factors for these two
954 nutrients' concentrations). As mentioned above, the differential control of anammox and
955 denitrification by substrate concentration may affect the observed ratio of the two rates in tracer
956 incubations. Tracer additions above ambient nutrient levels are necessary to detect a mass
957 spectrometric signal but often can result in rates above true in situ levels. Data on the kinetic
958 responses of anammox and denitrification are scarce, yet another area where further research
959 would be very useful.

960

961 **4.6 Possibility of N loss via AOA and other N cycling processes**

962 A recent paper (Kraft et al., 2022) reported that dense cultures of the ammonium
963 oxidizing archaea (AOA) *Nitrosopumilus maritimus* can support the O_2 dependent process of
964 NH_4^+ oxidation in deoxygenated waters via NO disproportionation to O_2 and N_2 . This
965 mechanism would be a third N loss process that, if occurring in OMZs, would be measured as
966 anammox or denitrification. In order to investigate the possible significance of this N loss
967 pathway in ODZ waters, we calculated the maximum possible N loss from NH_4^+ oxidation – the
968 N loss that would result if all of the $^{15}\text{N}\text{-NO}_2^-$ produced in our NH_4^+ oxidation experiments was

969 converted into N₂ via the proposed NO disproportionation reaction. These maximum NH₄⁺
970 oxidation derived N loss rates were a small fraction of the total N loss rates at most depths
971 (Supplementary Table S5). As a result, even these unrealistically high estimates of N₂
972 production from AOA do not suggest that AOA are significant agents for fixed N loss. The
973 depths where this was not the case are all either oxic or upper oxycline depths where NH₄⁺
974 oxidation rates peak and do not require NO disproportionation to supply O₂, or depths where
975 equally low NH₄⁺ oxidation, anammox, and denitrification rates would allow a higher percentage
976 of the total N loss to be due to NH₄⁺ oxidation. As a result, our calculation argues that N loss
977 derived from NH₄⁺ oxidation is not a significant N loss flux in ODZs. Thus, we argue that our
978 conclusions regarding the relative balance of anammox and denitrification, as well as the
979 relationship of these two N loss processes to other parts of the N cycle, do not need to be revised
980 to account for N loss via NO disproportionation in AOA.

981 We note that an additional N recycling pathway, dissimilatory nitrate/nitrite reduction to
982 ammonium (DNRA) can occur under low O₂ conditions similar to those preferred by anammox
983 and denitrification. While some OMZ studies have found rates and *nrfA* abundances comparable
984 to anammox, denitrification, and NH₄⁺ oxidation rates and marker gene abundances (Lam et al.,
985 2009; Jensen et al., 2011), DNRA is best described as an extremely variable process. Other past
986 OMZ studies have often found negligible rates (De Brabandere et al., 2014; Kalvelage et al.,
987 2013; Füssel et al., 2011) and little genetic evidence for DNRA (Kalvelage et al., 2013;
988 Fuchsman et al., 2017). Due to this variability we chose to focus this study on what are arguably
989 the most consistently relevant rates for OMZ N biogeochemistry.

990

991 **5 Conclusions**

992 Nitrogen is an essential component of life and as a result, its availability can function as a
993 cap on biological productivity in many marine ecosystems. Since all the ocean is linked through
994 an intricate web of currents that span the globe, the N biogeochemistry of small regions can
995 affect the biogeochemistry of the rest of the ocean. Although OMZs account for just 0.1 - 1% of
996 the ocean's total volume (Lam and Kuypers, 2011; Codispoti and Richards, 1976; Naqvi, 1987;
997 Bange et al., 2000; Codispoti et al., 2005) they account for 30-50% of all total marine N loss
998 (DeVries et al., 2013). As a result, developing an understanding of N cycling within OMZs is
999 critical for comprehending the total marine N budget. Here we presented measurements from the
1000 ETNP OMZ of five microbial N cycling metabolisms, all of which have NO_2^- as a product,
1001 reactant, or intermediate. Understanding the magnitudes of these rates is key to determining the
1002 OMZ inventory of N species as well as an important piece of understanding the marine N
1003 budget.

1004 Our results add to the growing evidence that the N recycling process of NO_3^- reduction is
1005 the largest OMZ N flux followed by the recycling process of NO_2^- oxidation back to NO_3^- .
1006 These two processes peaked in the oxycline or ODZ top and were usually much greater than the
1007 two N loss processes of anammox and denitrification, a departure from the established view that
1008 understanding N loss processes alone is the key to understanding OMZ biogeochemistry. We
1009 also add further evidence to the body of literature that supports the occurrence of anaerobic NO_2^-
1010 oxidation in OMZ regions, most strikingly through a series of O_2 manipulation experiments that
1011 show NO_2^- oxidation at putative O_2 concentrations as low as 1 nM. We conducted experiments
1012 on waters from two deoxygenated depths to evaluate if NO_2^- dismutation provides the oxidative
1013 power for observed anaerobic NO_2^- oxidation and found no evidence of NO_2^- dismutation except
1014 in one treatment – the closest to in situ NO_2^- conditions. Further exploration of the dismutation

1015 hypothesis might therefore usefully focus on conditions near in situ NO_2^- concentrations. Across
1016 our experiments, the percent of N loss due to anammox was consistently above the theoretical
1017 prediction of at most 29% anammox. Our observations that NO_3^- reduction and NO_2^- oxidation
1018 greatly surpass N loss, especially in shallow boundary waters, further reinforce the view that
1019 NO_2^- in the SNM is sourced from NO_3^- reduction.

1020 Together, these observations provide additional data that supports several new views of
1021 OMZ biogeochemistry. We hope that our work inspires additional isotopic experiments,
1022 culturing efforts, or genomic studies, especially those that seek to further test the occurrence of
1023 NO_2^- oxidation under functionally anoxic conditions and to examine alternative oxidants for this
1024 process. In addition, we emphasize the importance of integrating our experimental results into
1025 future OMZ N and C biogeochemical models, especially our results showing the predominance
1026 of NO_3^- reduction and NO_2^- oxidation over N loss. The development of an accurate model of
1027 OMZ N cycling is essential towards forecasting future changes in marine productivity and
1028 ecology as OMZs respond to climate change and other anthropogenic environmental changes.

1029

1030 **Author contributions**

1031 XS, CF and BBW designed, and CF performed, measured, and calculated the NO_3^- reduction and
1032 NH_4^+ oxidation rates. BBW and JCT designed, BBW and JCT performed, and JCT measured
1033 and calculated the anammox and denitrification depth profile experiments. BBW and XS
1034 designed, JCT, BBW, and XS performed, XS and KD measured, and KD, EW, and JCT
1035 calculated the NO_2^- oxidation depth profiles. TT and ARB designed, TT performed, DEM and
1036 JCT measured, and EW and JCT calculated the anammox and denitrification profiles from the
1037 FK180624 cruise. TT and ARB designed, and TT performed, measured, and calculated the NO_2^-

1038 oxidation O₂ variation experiments. ARB and TT designed, TT performed, EW, XS, and JCT
1039 measured, and EW and JCT calculated the dismutation experiments. SO provided critical help in
1040 running the mass spectrometer to measure all samples except the oxygen variation experiments.
1041 BBW performed the correlation and RDA analyses. JCT drafted the paper with inputs from all
1042 authors.

1043

1044 **Competing Interests**

1045 The authors declare that they have no conflicts of interest.

1046

1047 **Data Availability**

1048 All data discussed in this manuscript will be archived in Zenodo upon publication.

1049

1050 **Acknowledgments**

1051 We would like to acknowledge the crew and scientists of the R/V *Sally Ride* and the R/V *Falkor*
1052 for logistical and scientific support during our 2018 cruises. We thank Amal Jayakumar for
1053 providing *amoA* and *nirS* gene abundances for the RDA and PCA analyses. We thank Emilio
1054 Robledo-Garcia for assistance using the LUMOS sensor for the NO₂⁻ oxidation O₂ gradient
1055 experiments. We thank Matthias Spieler for supporting NO₃⁻ reduction rate measurements in
1056 Basel. We thank Patrick Boduch for his aid in reviewing graphics before submission. We also
1057 acknowledge the Schmidt Ocean Institute which provided R/V *Falkor* ship time to ARB. We
1058 thank the Simons Foundation and National Science Foundation for supporting ARB, TT, and
1059 DEM on Simons Foundation grant 622065 and NSF grants OCE-2138890 and OCE-2142998 as
1060 well as support for BBW, CF, JCT, and XS through NSF grant OCE-1657663.

1061

1062 **References**

1063 Anderson, J. J., Okubo, A., Robbins, A. S., and Richards, F. A.: A model for nitrate distributions
1064 in oceanic oxygen minimum zones, *Deep Sea Res. Part A. Oceanogr. Res. Pap.*, 29, 1113–1140,
1065 [https://doi.org/10.1016/0198-0149\(82\)90031-0](https://doi.org/10.1016/0198-0149(82)90031-0), 1982.

1066 ASTM International: *Standard Guide for Spiking into Aqueous Samples*, West Conshohocken,
1067 PA, 2006.

1068 Babbin, A. R., Keil, R. G., Devol, A. H., and Ward, B. B.: Organic matter stoichiometry, flux,
1069 and oxygen control nitrogen loss in the ocean, *Science (80-.)*, 344, 406–408,
1070 <https://doi.org/10.1126/science.1248364>, 2014.

1071 Babbin, A. R., Peters, B. D., Mordy, C. W., Widner, B., Casciotti, K. L., and Ward, B. B.:
1072 Multiple metabolisms constrain the anaerobic nitrite budget in the Eastern Tropical South
1073 Pacific, *Global Biogeochem. Cycles*, 31, 258–271, <https://doi.org/10.1002/2016GB005407>,
1074 2017.

1075 Babbin, A. R., Buchwald, C., Morel, F. M. M., Wankel, S. D., and Ward, B. B.: Nitrite oxidation
1076 exceeds reduction and fixed nitrogen loss in anoxic Pacific waters, *Mar. Chem.*, 224, 103814,
1077 <https://doi.org/10.1016/J.MARCHEM.2020.103814>, 2020.

1078 Bange, H. W., Rixen, T., Johansen, A. M., Siefert, R. L., Ramesh, R., Ittekkot, V., Hoffmann, M.
1079 R., and Andreae, M. O.: A revised nitrogen budget of the Arabian Sea, *Global Biogeochem.*
1080 *Cycles*, 14, 1283–1297, <https://doi.org/10.1029/1999GB001228>, 2000.

1081 Beman, J. M., Leilei Shih, J., and Popp, B. N.: Nitrite oxidation in the upper water column and
1082 oxygen minimum zone of the eastern tropical North Pacific Ocean, *ISME J.* 2013 711, 7, 2192–
1083 2205, <https://doi.org/10.1038/ismej.2013.96>, 2013.

1084 Berg, J. S., Ahmerkamp, S., Pjevac, P., Hausmann, B., Milucka, J., and Kuypers, M. M. M.:
1085 How low can they go? Aerobic respiration by microorganisms under apparent anoxia, *FEMS*
1086 *Microbiol. Rev.*, 46, 1–14, <https://doi.org/10.1093/FEMSRE/FUAC006>, 2022.

1087 Bianchi, D., Babbin, A. R., and Galbraith, E. D.: Enhancement of anammox by the excretion of
1088 diel vertical migrators, *Proc. Natl. Acad. Sci.*, 111, 15653–15658,
1089 <https://doi.org/10.1073/PNAS.1410790111>, 2014.

1090 Bock, E., Koops, H. P., Möller, U. C., and Rudert, M.: A new facultatively nitrite oxidizing
1091 bacterium, *Nitrobacter vulgaris* sp. nov., *Arch. Microbiol.* 1990 1532, 153, 105–110,
1092 <https://doi.org/10.1007/BF00247805>, 1990.

1093 De Brabandere, L., Canfield, D. E., Dalsgaard, T., Friederich, G. E., Revsbech, N. P., Ulloa, O.,
1094 and Thamdrup, B.: Vertical partitioning of nitrogen-loss processes across the oxic-anoxic
1095 interface of an oceanic oxygen minimum zone, *Environ. Microbiol.*, 16, 3041–3054,
1096 <https://doi.org/10.1111/1462-2920.12255>, 2014.

1097 Braman, R. S. and Hendrix, S. A.: Nanogram Nitrite and Nitrate Determination in Environmental
1098 and Biological Materials by Vanadium(III) Reduction with Chemiluminescence Detection, *Anal.*
1099 *Chem.*, 61, 2715–2718, 1989.

1100 Brandhorst, W.: Nitrification and Denitrification in the Eastern Tropical North Pacific, *J. du*
1101 *Cons. Cons. Perm. Int. pour l’exploration la mer*, 25, 3–20, 1959.

1102 Bristow, L. A., Dalsgaard, T., Tiano, L., Mills, D. B., Bertagnolli, A. D., Wright, J. J., Hallam, S.
1103 J., Ulloa, O., Canfield, D. E., Revsbech, N. P., and Thamdrup, B.: Ammonium and nitrite
1104 oxidation at nanomolar oxygen concentrations in oxygen minimum zone waters, *Proc. Natl.*
1105 *Acad. Sci. U. S. A.*, 113, 10601–10606, <https://doi.org/10.1073/PNAS.1600359113>, 2016.

1106 Bristow, L. A., Callbeck, C. M., Larsen, M., Altabet, M. A., Dekaezemacker, J., Forth, M.,

1107 Gauns, M., Glud, R. N., Kuypers, M. M. M., Lavik, G., Milucka, J., Naqvi, S. W. A., Pratihary,
1108 A., Revsbech, N. P., Thamdrup, B., Treusch, A. H., and Canfield, D. E.: N₂ production rates
1109 limited by nitrite availability in the Bay of Bengal oxygen minimum zone, *Nat. Geosci.*, 10, 24–
1110 29, <https://doi.org/10.1038/ngeo2847>, 2017.

1111 Buchwald, C. and Wankel, S. D.: Enzyme-catalyzed isotope equilibrium: A hypothesis to
1112 explain apparent N cycling phenomena in low oxygen environments, *Mar. Chem.*, 244, 104140,
1113 <https://doi.org/10.1016/J.MARCHEM.2022.104140>, 2022.

1114 Buchwald, C., Santoro, A. E., Stanley, R. H. R., and Casciotti, K. L.: Nitrogen cycling in the
1115 secondary nitrite maximum of the eastern tropical North Pacific off Costa Rica, *Global*
1116 *Biogeochem. Cycles*, 29, 2061–2081, <https://doi.org/10.1002/2015GB005187>, 2015.

1117 Bulow, S. E., Rich, J. J., Naik, H. S., Pratihary, A. K., and Ward, B. B.: Denitrification exceeds
1118 anammox as a nitrogen loss pathway in the Arabian Sea oxygen minimum zone, *Deep Sea Res.*
1119 *Part I Oceanogr. Res. Pap.*, 57, 384–393, <https://doi.org/10.1016/J.DSR.2009.10.014>, 2010.

1120 Busecke, J. J. M., Resplandy, L., Ditkovsky, S. J., and John, J. G.: Diverging Fates of the Pacific
1121 Ocean Oxygen Minimum Zone and Its Core in a Warming World, *AGU Adv.*, 3,
1122 e2021AV000470, <https://doi.org/10.1029/2021AV000470>, 2022.

1123 Casciotti, K. L.: Inverse kinetic isotope fractionation during bacterial nitrite oxidation, *Geochim.*
1124 *Cosmochim. Acta*, 73, 2061–2076, <https://doi.org/10.1016/J.GCA.2008.12.022>, 2009.

1125 Casciotti, K. L., Buchwald, C., and McIlvin, M.: Implications of nitrate and nitrite isotopic
1126 measurements for the mechanisms of nitrogen cycling in the Peru oxygen deficient zone, *Deep*
1127 *Sea Res. Part I Oceanogr. Res. Pap.*, 80, 78–93, <https://doi.org/10.1016/J.DSR.2013.05.017>,
1128 2013.

1129 Codispoti, L. A. and Packard, T. T.: Denitrification rates in the eastern tropical South Pacific, *J.*

1130 Mar. Res., 38, 453–477, 1980.

1131 Codispoti, L. A. and Richards, F. A.: An analysis of the horizontal regime of denitrification in
1132 the eastern tropical North Pacific, *Limnol. Oceanogr.*, 21, 379–388,
1133 <https://doi.org/10.4319/LO.1976.21.3.0379>, 1976.

1134 Codispoti, L. A., Brandes, J. A., Christensen, J. P., Devol, A. H., Naqvi, S. W. A., Paerl, H. W.,
1135 and Yoshinari, T.: The oceanic fixed nitrogen and nitrous oxide budgets: Moving targets as we
1136 enter the anthropocene?, *Sci. Mar.*, 65, 85–105, <https://doi.org/10.3989/SCIMAR.2001.65S285>,
1137 2001.

1138 Codispoti, L. A., Yoshinari, T., and Devol, A. H.: Suboxic respiration in the oceanic water
1139 column, in: *Respiration in Aquatic Ecosystems*, edited by: del Giorgio, P. A. and Williams, P. J.
1140 L., Oxford University Press, 225–247, 2005.

1141 Cram, J. A., Fuchsman, C. A., Duffy, M. E., Pretty, J. L., Lekanoff, R. M., Neibauer, J. A.,
1142 Leung, S. W., Huebert, K. B., Weber, T. S., Bianchi, D., Evans, N., Devol, A. H., Keil, R. G.,
1143 and McDonnell, A. M. P.: Slow Particle Remineralization, Rather Than Suppressed
1144 Disaggregation, Drives Efficient Flux Transfer Through the Eastern Tropical North Pacific
1145 Oxygen Deficient Zone, *Global Biogeochem. Cycles*, 36, e2021GB007080,
1146 <https://doi.org/10.1029/2021GB007080>, 2022.

1147 Dalsgaard, T., Canfield, D. E., Peterson, J., Thamdrup, B., and Acuna-Gonzales, J.: N production
1148 by anamox in the anoxic water column of Golfo Dulce, Costa Rica., *Nature*, 422, 606–608,
1149 <https://doi.org/10.1038/nature01526>, 2003.

1150 Dalsgaard, T., Thamdrup, B., Farías, L., and Revsbech, N. P.: Anammox and denitrification in
1151 the oxygen minimum zone of the eastern South Pacific, *Limnol. Oceanogr.*, 57, 1331–1346,
1152 <https://doi.org/10.4319/lo.2012.57.5.1331>, 2012.

1153 DeVries, T., Deutsch, C., Rafter, P. A., and Primeau, F.: Marine denitrification rates determined
1154 from a global 3-D inverse model, *Biogeosciences*, 10, 2481–2496, [https://doi.org/10.5194/BG-](https://doi.org/10.5194/BG-10-2481-2013)
1155 10-2481-2013, 2013.

1156 Freitag, A., Rudert, M., and Bock, E.: Growth of *Nitrobacter* by dissimilatoric nitrate reduction,
1157 *FEMS Microbiol. Lett.*, 48, 105–109, <https://doi.org/10.1111/J.1574-6968.1987.TB02524.X>,
1158 1987.

1159 Frey, C., Bange, H. W., Achterberg, E. P., Jayakumar, A., Löscher, C. R., Arévalo-Martínez, D.
1160 L., León-Palmero, E., Sun, M., Sun, X., Xie, R. C., Oleynik, S., and Ward, B. B.: Regulation of
1161 nitrous oxide production in low-oxygen waters off the coast of Peru, *Biogeosciences*, 17, 2263–
1162 2287, <https://doi.org/10.5194/BG-17-2263-2020>, 2020.

1163 Frey, C., Sun, X., Szemberski, L., Casciotti, K. L., Garcia-Robledo, E., Jayakumar, A., Kelly, C.
1164 L., and Lehmann, M. F.: Nitrous oxide production kinetics from ammonia oxidation in the
1165 Eastern Tropical North Pacific, *Limnol. Oceanogr.*, Under review, 2022.

1166 Fuchsman, C. A., Devol, A. H., Saunders, J. K., McKay, C., and Rocap, G.: Niche partitioning of
1167 the N cycling microbial community of an offshore oxygen deficient zone, *Front. Microbiol.*, 8,
1168 2384, <https://doi.org/10.3389/FMICB.2017.02384/BIBTEX>, 2017.

1169 Fuchsman, C. A., Palevsky, H. I., Widner, B., Duffy, M., Carlson, M. C. G., Neibauer, J. A.,
1170 Mulholland, M. R., Keil, R. G., Devol, A. H., and Rocap, G.: Cyanobacteria and cyanophage
1171 contributions to carbon and nitrogen cycling in an oligotrophic oxygen-deficient zone, *ISME J.*
1172 2019 1311, 13, 2714–2726, <https://doi.org/10.1038/s41396-019-0452-6>, 2019.

1173 Füssel, J., Lam, P., Lavik, G., Jensen, M. M., Holtappels, M., Günter, M., and Kuypers, M. M.
1174 M.: Nitrite oxidation in the Namibian oxygen minimum zone, *ISME J.*, 6, 1200–1209,
1175 <https://doi.org/10.1038/ismej.2011.178>, 2011.

1176 Füssel, J., Lücker, S., Yilmaz, P., Nowka, B., van Kessel, M. A. H. J., Bourceau, P., Hach, P. F.,
1177 Littmann, S., Berg, J., Spieck, E., Daims, H., Kuypers, M. M. M., and Lam, P.: Adaptability as
1178 the key to success for the ubiquitous marine nitrite oxidizer *Nitrococcus*, *Sci. Adv.*, 3,
1179 https://doi.org/10.1126/SCIADV.1700807/SUPPL_FILE/1700807_TABLES1_TO_S10.ZIP,
1180 2017.

1181 Ganesh, S., Parris, D. J., Delong, E. F., and Stewart, F. J.: Metagenomic analysis of size-
1182 fractionated picoplankton in a marine oxygen minimum zone, *ISME J.* 2014 81, 8, 187–211,
1183 <https://doi.org/10.1038/ismej.2013.144>, 2013.

1184 Ganesh, S., Bristow, L. A., Larsen, M., Sarode, N., Thamdrup, B., and Stewart, F. J.: Size-
1185 fraction partitioning of community gene transcription and nitrogen metabolism in a marine
1186 oxygen minimum zone, *ISME J.* 2015 912, 9, 2682–2696, <https://doi.org/10.1038/ismej.2015.44>,
1187 2015.

1188 Garcia-Robledo, E., Borisov, S., Klimant, I., and Revsbech, N. P.: Determination of respiration
1189 rates in water with sub-micromolar oxygen concentrations, *Front. Mar. Sci.*, 3, 244,
1190 <https://doi.org/10.3389/FMARS.2016.00244/BIBTEX>, 2016.

1191 Garcia-Robledo, E., Padilla, C. C., Aldunate, M., Stewart, F. J., Ulloa, O., Paulmier, A., Gregori,
1192 G., and Revsbech, N. P.: Cryptic oxygen cycling in anoxic marine zones, *Proc. Natl. Acad. Sci.*
1193 *U. S. A.*, 114, 8319–8324, <https://doi.org/10.1073/PNAS.1619844114>, 2017.

1194 Garcia-Robledo, E., Paulmier, A., Borisov, S. M., and Revsbech, N. P.: Sampling in low oxygen
1195 aquatic environments: The deviation from anoxic conditions, *Limnol. Oceanogr. Methods*, 19,
1196 733–740, <https://doi.org/10.1002/LOM3.10457>, 2021.

1197 Granger, J., & Sigman, D. M.: Removal of nitrite with sulfamic acid for nitrate N and O isotope
1198 analysis with the denitrifier method, *Rapid Commun. Mass Spectrom.*, 23, 3753–3762., *Rapid*

1199 Commun. Mass Spectrom., 23, 3753–3762, <https://doi.org/10.1002/rcm>, 2009.

1200 Granger, J. and Wankel, S. D.: Isotopic overprinting of nitrification on denitrification as a
1201 ubiquitous and unifying feature of environmental nitrogen cycling, Proc. Natl. Acad. Sci. U. S.
1202 A., 113, E6391–E6400,
1203 https://doi.org/10.1073/PNAS.1601383113/SUPPL_FILE/PNAS.201601383SI.PDF, 2016.

1204 Hamersley, M. R., Lavik, G., Woebken, D., Rattray, J. E., Lam, P., Hopmans, E. C., Sinninghe
1205 Damsté, J. S., Krüger, S., Graco, M., Gutiérrez, D., and Kuypers, M. M. M.: Anaerobic
1206 ammonium oxidation in the Peruvian oxygen minimum zone, Limnol. Oceanogr., 52, 923–933,
1207 <https://doi.org/10.4319/LO.2007.52.3.0923>, 2007.

1208 Holmes, R. M., Aminot, A., Kérouel, R., Hooker, B. A., and Peterson, B. J.: A simple and
1209 precise method for measuring ammonium in marine and freshwater ecosystems, Can. J. Fish.
1210 Aquat. Sci., 56, 1801–1808, <https://doi.org/10.1139/f99-128>, 1999.

1211 Horak, R. E. A., Ruef, W., Ward, B. B., and Devol, A. H.: Expansion of denitrification and
1212 anoxia in the eastern tropical North Pacific from 1972 to 2012, Geophys. Res. Lett., 43, 5252–
1213 5260, <https://doi.org/10.1002/2016GL068871>, 2016.

1214 Ito, T., Minobe, S., Long, M. C., and Deutsch, C.: Upper ocean O₂ trends: 1958–2015, Geophys.
1215 Res. Lett., 44, 4214–4223, <https://doi.org/10.1002/2017GL073613>, 2017.

1216 Jayakumar, A., Wajih, S., Naqvi, A., and Ward, B. B.: Distribution and Relative Quantification
1217 of Key Genes Involved in Fixed Nitrogen Loss From the Arabian Sea Oxygen Minimum Zone,
1218 Indian Ocean Biogeochem. Process. Ecol. Var. Geophys. Monogr. Ser., 185,
1219 <https://doi.org/10.1029/2008GM000730>, 2009.

1220 Jensen, M. M., Lam, P., Revsbech, N. P., Nagel, B., Gaye, B., Jetten, M. S. M., and Kuypers, M.
1221 M. M.: Intensive nitrogen loss over the Omani Shelf due to anammox coupled with dissimilatory

1222 nitrite reduction to ammonium, *ISME J.* 2011 510, 5, 1660–1670,
1223 <https://doi.org/10.1038/ismej.2011.44>, 2011.

1224 Kalvelage, T., Lavik, G., Lam, P., Contreras, S., Arteaga, L., Löscher, C. R., Oschlies, A.,
1225 Paulmier, A., Stramma, L., and M Kuypers, M. M.: Nitrogen cycling driven by organic matter
1226 export in the South Pacific oxygen minimum zone, 55812, <https://doi.org/10.1038/NGEO1739>,
1227 2013.

1228 Keeling, R. F., Körtzinger, A., and Gruber, N.: Ocean deoxygenation in a warming world, *Ann.*
1229 *Rev. Mar. Sci.*, 2, 199–229, <https://doi.org/10.1146/annurev.marine.010908.163855>, 2010.

1230 Kemeny, P. C., Weigand, M. A., Zhang, R., Carter, B. R., Karsh, K. L., Fawcett, S. E., and
1231 Sigman, D. M.: Enzyme-level interconversion of nitrate and nitrite in the fall mixed layer of the
1232 Antarctic Ocean, *Global Biogeochem. Cycles*, 30, 1069–1085,
1233 <https://doi.org/10.1002/2015GB005350>, 2016.

1234 Kirstein, K. and Bock, E.: Close genetic relationship between *Nitrobacter hamburgensis* nitrite
1235 oxidoreductase and *Escherichia coli* nitrate reductases, *Arch. Microbiol.* 1993 1606, 160, 447–
1236 453, <https://doi.org/10.1007/BF00245305>, 1993.

1237 Koch, H., Lücker, S., Albertsen, M., Kitzinger, K., Herbold, C., Spieck, E., Nielsen, P. H.,
1238 Wagner, M., and Daims, H.: Expanded metabolic versatility of ubiquitous nitrite-oxidizing
1239 bacteria from the genus *Nitrospira*, *Proc. Natl. Acad. Sci. U. S. A.*, 112, 11371–11376,
1240 <https://doi.org/10.1073/PNAS.1506533112>, 2015.

1241 Kondo, Y. and Moffett, J. W.: Iron redox cycling and subsurface offshore transport in the eastern
1242 tropical South Pacific oxygen minimum zone, *Mar. Chem.*, 168, 95–103,
1243 <https://doi.org/10.1016/J.MARCHEM.2014.11.007>, 2015.

1244 Kraft, B., Jehmlich, N., Larsen, M., Bristow, L. A., Könneke, M., Thamdrup, B., and Canfield,

1245 D. E.: Oxygen and nitrogen production by an ammonia-oxidizing archaeon, *Science* (80-.), 375,
1246 97–100,
1247 https://doi.org/10.1126/SCIENCE.ABE6733/SUPPL_FILE/SCIENCE.ABE6733_MDAR_REPR
1248 [ODUCIBILITY_CHECKLIST.PDF](https://doi.org/10.1126/SCIENCE.ABE6733/SUPPL_FILE/SCIENCE.ABE6733_MDAR_REPR), 2022.

1249 Kuenen, J. G.: Anammox bacteria from discovery, 6, <https://doi.org/10.1038/nrmicro1857>, 2008.

1250 Kuypers, M. M. M., Lavik, G., Woebken, D., Schmid, M., Fuchs, B. M., Amann, R., Jørgensen,
1251 B. B., and Jetten, M. S. M.: Massive nitrogen loss from the Benguela upwelling system through
1252 anaerobic ammonium oxidation, *Proc. Natl. Acad. Sci. U. S. A.*, 102, 6478–6483,
1253 <https://doi.org/10.1073/PNAS.0502088102>, 2005.

1254 Lam, P. and Kuypers, M. M. M.: Microbial Nitrogen Cycling Processes in Oxygen Minimum
1255 Zones, *Ann. Rev. Mar. Sci.*, 3, 317–345, <https://doi.org/10.1146/annurev-marine-120709->
1256 [142814](https://doi.org/10.1146/annurev-marine-120709-), 2011.

1257 Lam, P., Lavik, G., Jensen, M. M., Van Vossenberg, J. De, Schmid, M., Woebken, D., Gutiérrez,
1258 D., Amann, R., Jetten, M. S. M., and Kuypers, M. M. M.: Revising the nitrogen cycle in the
1259 Peruvian oxygen minimum zone, *Proc. Natl. Acad. Sci. U. S. A.*, 106, 4752–4757,
1260 <https://doi.org/10.1073/PNAS.0812444106>, 2009.

1261 Lam, P., Jensen, M. M., Kock, A., Lettmann, K. A., Plancherel, Y., Lavik, G., Bange, H. W., and
1262 Kuypers, M. M. M.: Origin and fate of the secondary nitrite maximum in the Arabian Sea,
1263 *Biogeosciences*, 8, 1565–1577, <https://doi.org/10.5194/BG-8-1565-2011>, 2011.

1264 Van de Leemput, I. A., Veraart, A. J., Dakos, V., De Klein, J. J. M., Strous, M., and Scheffer,
1265 M.: Predicting microbial nitrogen pathways from basic principles, *Environ. Microbiol.*, 13,
1266 1477–1487, <https://doi.org/10.1111/J.1462-2920.2011.02450.X>, 2011.

1267 Lehner, P., Larndorfer, C., Garcia-Robledo, E., Larsen, M., Borisov, S. M., Revsbech, N. P.,

1268 Glud, R. N., Canfield, D. E., and Klimant, I.: LUMOS - A Sensitive and Reliable Optode System
1269 for Measuring Dissolved Oxygen in the Nanomolar Range, *PLoS One*, 10, e0128125,
1270 <https://doi.org/10.1371/JOURNAL.PONE.0128125>, 2015.

1271 Lipschultz, F., Wofsy, S. C., Ward, B. B., Codispoti, L. A., Friedrich, G., and Elkins, J. W.:
1272 Bacterial transformations of inorganic nitrogen in the oxygen-deficient waters of the Eastern
1273 Tropical South Pacific Ocean, *Deep Sea Res. Part A. Oceanogr. Res. Pap.*, 37, 1513–1541,
1274 [https://doi.org/10.1016/0198-0149\(90\)90060-9](https://doi.org/10.1016/0198-0149(90)90060-9), 1990.

1275 Lomas, M. W. and Lipschultz, F.: Forming the primary nitrite maximum: Nitrifiers or
1276 phytoplankton?, *Limnol. Oceanogr.*, 51, 2453–2467, <https://doi.org/10.4319/LO.2006.51.5.2453>,
1277 2006.

1278 Luther, G. W.: The role of one- and two-electron transfer reactions in forming
1279 thermodynamically unstable intermediates as barriers in multi-electron redox reactions, *Aquat.*
1280 *Geochemistry*, 16, 395–420, <https://doi.org/10.1007/S10498-009-9082-3/FIGURES/14>, 2010.

1281 Luther, G. W. and Popp, J. I.: Kinetics of the Abiotic Reduction of Polymeric Manganese
1282 Dioxide by Nitrite: An Anaerobic Nitrification Reaction, *Aquat. Geochemistry* 2002 81, 8, 15–
1283 36, <https://doi.org/10.1023/A:1020325604920>, 2002.

1284 Margolskee, A., Frenzel, H., Emerson, S., and Deutsch, C.: Ventilation Pathways for the North
1285 Pacific Oxygen Deficient Zone, *Global Biogeochem. Cycles*, 33, 875–890,
1286 <https://doi.org/10.1029/2018GB006149>, 2019.

1287 Martin, J. H., Knauer, G. A., Karl, D. M., and Broenkow, W. W.: VERTEX: carbon cycling in
1288 the northeast Pacific, *Deep Sea Res. Part A. Oceanogr. Res. Pap.*, 34, 267–285,
1289 [https://doi.org/10.1016/0198-0149\(87\)90086-0](https://doi.org/10.1016/0198-0149(87)90086-0), 1987.

1290 McIlvin, M. R. and Altabet, M. A.: Chemical conversion of nitrate and nitrite to nitrous oxide for

1291 nitrogen and oxygen isotopic analysis in freshwater and seawater, *Anal. Chem.*, 77, 5589–5595,
1292 <https://doi.org/10.1021/ac050528s>, 2005.

1293 Mincer, T. J., Church, M. J., Taylor, L. T., Preston, C., Karl, D. M., and DeLong, E. F.:
1294 Quantitative distribution of presumptive archaeal and bacterial nitrifiers in Monterey Bay and the
1295 North Pacific Subtropical Gyre, *Environ. Microbiol.*, 9, 1162–1175,
1296 <https://doi.org/10.1111/J.1462-2920.2007.01239.X>, 2007.

1297 Monreal, P. J., Kelly, C. L., Travis, N. M., and Casciotti, K. L.: Identifying the Sources and
1298 Drivers of Nitrous Oxide Accumulation in the Eddy-Influenced Eastern Tropical North Pacific
1299 Oxygen-Deficient Zone, *Global Biogeochem. Cycles*, 36, e2022GB007310,
1300 <https://doi.org/10.1029/2022GB007310>, 2022.

1301 Moriyasu, R., Evans, N., Bolster, K. M., Hardisty, D. S., and Moffett, J. W.: The Distribution
1302 and Redox Speciation of Iodine in the Eastern Tropical North Pacific Ocean, *Global
1303 Biogeochem. Cycles*, 34, e2019GB006302, <https://doi.org/10.1029/2019GB006302>, 2020.

1304 Naqvi, S. W. A.: Some aspects of the oxygen-deficient conditions and denitrification in the
1305 Arabian Sea, *J. Mar. Res.*, 45, 1049–1072, 1987.

1306 Nozaki, Y.: A fresh look at element distribution in the North Pacific Ocean, *Eos, Trans. Am.
1307 Geophys. Union*, 78, 221–221, <https://doi.org/10.1029/97EO00148>, 1997.

1308 Oshiki, M., Satoh, H., and Okabe, S.: Ecology and physiology of anaerobic ammonium oxidizing
1309 bacteria, *Environ. Microbiol.*, 18, 2784–2796, [https://doi.org/10.1111/1462-
1310 2920.13134/SUPPINFO](https://doi.org/10.1111/1462-2920.13134/SUPPINFO), 2016.

1311 Padilla, C. C., Bristow, L. A., Sarode, N., Garcia-Robledo, E., Gómez Ramírez, E., Benson, C.
1312 R., Bourbonnais, A., Altabet, M. A., Girguis, P. R., Thamdrup, B., and Stewart, F. J.: NC10
1313 bacteria in marine oxygen minimum zones, *ISME J.* 2016 108, 10, 2067–2071,

1314 <https://doi.org/10.1038/ismej.2015.262>, 2016.

1315 Peng, X., Fuchsman, C. A., Jayakumar, A., Oleynik, S., Martens-Habbena, W., Devol, A. H., and
1316 Ward, B. B.: Ammonia and nitrite oxidation in the Eastern Tropical North Pacific, *Global*
1317 *Biogeochem. Cycles*, 29, 2034–2049, <https://doi.org/10.1002/2015GB005278>, 2015.

1318 Peng, X., Fuchsman, C. A., Jayakumar, A., Warner, M. J., Devol, A. H., and Ward, B. B.:
1319 Revisiting nitrification in the Eastern Tropical South Pacific: A focus on controls, *J. Geophys.*
1320 *Res. Ocean.*, 121, 1667–1684, <https://doi.org/10.1002/2015JC011455>, 2016.

1321 Penn, J., Weber, T., and Deutsch, C.: Microbial functional diversity alters the structure and
1322 sensitivity of oxygen deficient zones, *Geophys. Res. Lett.*, 43, 9773–9780,
1323 <https://doi.org/10.1002/2016GL070438>, 2016.

1324 Peters, B. D., Babbin, A. R., Lettmann, K. A., Mordy, C. W., Ulloa, O., Ward, B. B., and
1325 Casciotti, K. L.: Vertical modeling of the nitrogen cycle in the eastern tropical South Pacific
1326 oxygen deficient zone using high-resolution concentration and isotope measurements, *Global*
1327 *Biogeochem. Cycles*, 30, 1661–1681, <https://doi.org/10.1002/2016GB005415>, 2016.

1328 R: A language and environment for statistical computing:
1329 Starkenburg, S. R., Larimer, F. W., Stein, L. Y., Klotz, M. G., Chain, P. S. G., Sayavedra-Soto,
1330 L. A., Poret-Peterson, A. T., Gentry, M. E., Arp, D. J., Ward, B., and Bottomley, P. J.: Complete
1331 genome sequence of *Nitrobacter hamburgensis* X14 and comparative genomic analysis of
1332 species within the genus *Nitrobacter*, *Appl. Environ. Microbiol.*, 74, 2852–2863,
1333 https://doi.org/10.1128/AEM.02311-07/SUPPL_FILE/SUPPLEMENTAL_TABLE_2.PDF,
1334 2008.

1335 Stramma, L., Johnson, G. C., Sprintall, J., and Mohrholz, V.: Expanding oxygen-minimum zones
1336 in the tropical oceans, *Science (80-.)*, 320, 655–658,

1337 <https://doi.org/10.1126/SCIENCE.1153847/ASSET/09F7EF41-9228-40BD-8E17->
1338 [06C4E9218CC5/ASSETS/GRAPHIC/320_655_F2.JPEG](https://doi.org/10.1126/SCIENCE.1153847/ASSET/09F7EF41-9228-40BD-8E17-06C4E9218CC5/ASSETS/GRAPHIC/320_655_F2.JPEG), 2008.

1339 Strickland, J. D. H. and Parsons, T. R.: A Practical Handbook of Seawater Analysis, Fisheries
1340 Research Board of Canada, Ottawa, 1972.

1341 Strohm, T. O., Griffin, B., Zumft, W. G., and Schink, B.: Growth yields in bacterial
1342 denitrification and nitrate ammonification, *Appl. Environ. Microbiol.*, 73, 1420–1424,
1343 <https://doi.org/10.1128/AEM.02508-06/ASSET/88AA1997-7BB3-42B6-A761->
1344 [DCB47D972CA6/ASSETS/GRAPHIC/ZAM0050775730001.JPEG](https://doi.org/10.1128/AEM.02508-06/ASSET/88AA1997-7BB3-42B6-A761-DCB47D972CA6/ASSETS/GRAPHIC/ZAM0050775730001.JPEG), 2007.

1345 Strous, M., Heijnen, J. J., Kuenen, J. G., and Jetten, M. S. M.: The sequencing batch reactor as a
1346 powerful tool for the study of slowly growing anaerobic ammonium-oxidizing microorganisms,
1347 *Appl. Microbiol. Biotechnol.* 1998 505, 50, 589–596, <https://doi.org/10.1007/S002530051340>,
1348 1998.

1349 Sun, X. and Ward, B. B.: Novel metagenome-assembled genomes involved in the nitrogen cycle
1350 from a Pacific oxygen minimum zone, *ISME Commun.* 2021 11, 1, 1–5,
1351 <https://doi.org/10.1038/s43705-021-00030-2>, 2021.

1352 Sun, X., Ji, Q., Jayakumar, A., and Ward, B. B.: Dependence of nitrite oxidation on nitrite and
1353 oxygen in low-oxygen seawater, *Geophys. Res. Lett.*, 44, 7883–7891,
1354 <https://doi.org/10.1002/2017GL074355>, 2017.

1355 Sun, X., Kop, L. F. M., Lau, M. C. Y., Frank, J., Jayakumar, A., Lückner, S., and Ward, B. B.:
1356 Uncultured Nitrospina-like species are major nitrite oxidizing bacteria in oxygen minimum
1357 zones, *ISME J.*, <https://doi.org/10.1038/s41396-019-0443-7>, 2019.

1358 Sun, X., Frey, C., Garcia-Robledo, E., Jayakumar, A., and Ward, B. B.: Microbial niche
1359 differentiation explains nitrite oxidation in marine oxygen minimum zones, *ISME J.* 2021 155,

1360 15, 1317–1329, <https://doi.org/10.1038/s41396-020-00852-3>, 2021.

1361 Sun, X., Frey, C., and Ward, B. B.: Nitrite Oxidation Across the Full Oxygen Spectrum in the
1362 Ocean, *Global Biogeochem. Cycles*, 37, e2022GB007548,
1363 <https://doi.org/10.1029/2022GB007548>, 2023.

1364 Suter, E. A., Scranton, M. I., Chow, S., Stinton, D., Medina Faull, L., and Taylor, G. T.: Niskin
1365 bottle sample collection aliases microbial community composition and biogeochemical
1366 interpretation, *Limnol. Oceanogr.*, 62, 606–617, <https://doi.org/10.1002/LNO.10447>, 2017.

1367 Tang, W., Tracey, J. C., Carroll, J., Wallace, E., Lee, J. A., Nathan, L., Sun, X., Jayakumar, A.,
1368 and Ward, B. B.: Nitrous oxide production in the Chesapeake Bay, *Limnol. Oceanogr.*, 67,
1369 2101–2116, <https://doi.org/10.1002/LNO.12191>, 2022.

1370 Taylor, B. W., Keep, C. F., Hall, R. O., Koch, B. J., Tronstad, L. M., Flecker, A. S., and Ulseth,
1371 A. J.: Improving the fluorometric ammonium method: matrix effects, background fluorescence,
1372 and standard additions, *Am. Benthol. Soc.*, 26, 167–177, <https://doi.org/10.1899/0887-3593>,
1373 2007.

1374 Thamdrup, B. and Dalsgaard, T.: The fate of ammonium in anoxic manganese oxide-rich marine
1375 sediment, *Geochim. Cosmochim. Acta*, 64, 4157–4164, <https://doi.org/10.1016/S0016->
1376 [7037\(00\)00496-8](https://doi.org/10.1016/S0016-7037(00)00496-8), 2000.

1377 Thamdrup, B. and Dalsgaard, T.: Production of N₂ through anaerobic ammonium oxidation
1378 coupled to nitrate reduction in marine sediments, *Appl. Environ. Microbiol.*, 68, 1312–1318,
1379 <https://doi.org/10.1128/AEM.68.3.1312-1318.2002/ASSET/F1579424-64C0-464C-AF9C->
1380 [5BEB3458C869/ASSETS/GRAPHIC/AM0321630005.JPEG](https://doi.org/10.1128/AEM.68.3.1312-1318.2002/ASSET/F1579424-64C0-464C-AF9C-5BEB3458C869/ASSETS/GRAPHIC/AM0321630005.JPEG), 2002.

1381 Thamdrup, B., Dalsgaard, T., Jensen, M. M., Ulloa, O., Fariás, L., and Escribano, R.: Anaerobic
1382 ammonium oxidation in the oxygen-deficient waters off northern Chile, *Limnol. Oceanogr.*, 51,

1383 2145–2156, <https://doi.org/10.4319/LO.2006.51.5.2145>, 2006.

1384 Tiano, L., Garcia-Robledo, E., Dalsgaard, T., Devol, A. H., Ward, B. B., Ulloa, O., Canfield, D.
1385 E., and Peter Revsbech, N.: Oxygen distribution and aerobic respiration in the north and south
1386 eastern tropical Pacific oxygen minimum zones, *Deep Sea Res. Part I Oceanogr. Res. Pap.*, 94,
1387 173–183, <https://doi.org/10.1016/J.DSR.2014.10.001>, 2014.

1388 Tsementzi, D., Wu, J., Deutsch, S., Nath, S., Rodriguez-R, L. M., Burns, A. S., Ranjan, P.,
1389 Sarode, N., Malmstrom, R. R., Padilla, C. C., Stone, B. K., Bristow, L. A., Larsen, M., Glass, J.
1390 B., Thamdrup, B., Woyke, T., Konstantinidis, K. T., and Stewart, F. J.: SAR11 bacteria linked to
1391 ocean anoxia and nitrogen loss, *Nature*, 536, 179–183, <https://doi.org/10.1038/nature19068>,
1392 2016.

1393 Ulloa, O., Canfield, D. E., DeLong, E. F., Letelier, R. M., and Stewart, F. J.: Microbial
1394 oceanography of anoxic oxygen minimum zones, *Proc. Natl. Acad. Sci. U. S. A.*, 109, 15996–
1395 16003, <https://doi.org/10.1073/PNAS.1205009109>, 2012.

1396 Vedamati, J., Chan, C., and Moffett, J. W.: Distribution of dissolved manganese in the Peruvian
1397 Upwelling and Oxygen Minimum Zone, *Geochim. Cosmochim. Acta*, 156, 222–240,
1398 <https://doi.org/10.1016/J.GCA.2014.10.026>, 2015.

1399 Wanninkhof, R.: Relationship between wind speed and gas exchange over the ocean, *J. Geophys.*
1400 *Res. Ocean.*, 97, 7373–7382, <https://doi.org/10.1029/92JC00188>, 1992.

1401 Ward, B. B., Glover, H. E., and Lipschultz, F.: Chemoautotrophic activity and nitrification in the
1402 oxygen minimum zone off Peru, *Deep Sea Res. Part A. Oceanogr. Res. Pap.*, 36, 1031–1051,
1403 [https://doi.org/10.1016/0198-0149\(89\)90076-9](https://doi.org/10.1016/0198-0149(89)90076-9), 1989.

1404 Ward, B. B., Tuit, C. B., Jayakumar, A., Rich, J. J., Moffett, J., and Naqvi, S. W. A.: Organic
1405 carbon, and not copper, controls denitrification in oxygen minimum zones of the ocean, *Deep*

1406 Sea Res. Part I Oceanogr. Res. Pap., 55, 1672–1683, <https://doi.org/10.1016/J.DSR.2008.07.005>,
1407 2008.

1408 Ward, B. B., Devol, A. H., Rich, J. J., Chang, B. X., Bulow, S. E., Naik, H., Pratihary, A., and
1409 Jayakumar, A.: Denitrification as the dominant nitrogen loss process in the Arabian Sea, Nat.
1410 2009 4617260, 461, 78–81, <https://doi.org/10.1038/nature08276>, 2009.

1411 Weigand, M. A., Foriel, J., Barnett, B., Oleynik, S., and Sigman, D. M.: Updates to
1412 instrumentation and protocols for isotopic analysis of nitrate by the denitrifier method, Rapid
1413 Commun. Mass Spectrom., 30, 1365–1383, <https://doi.org/10.1002/rcm.7570>, 2016.

1414 Wunderlich, A., Meckenstock, R. U., and Einsiedl, F.: A mixture of nitrite-oxidizing and
1415 denitrifying microorganisms affects the $\delta^{18}\text{O}$ of dissolved nitrate during anaerobic microbial
1416 denitrification depending on the $\delta^{18}\text{O}$ of ambient water, Geochim. Cosmochim. Acta, 119, 31–
1417 45, <https://doi.org/10.1016/J.GCA.2013.05.028>, 2013.

1418